

Variable-Stepsize Implicit Peer Triplets in ODE Constrained Optimal Control

Jens Lang

*Technical University Darmstadt, Department of Mathematics
Dolivostraße 15, 64293 Darmstadt, Germany
lang@mathematik.tu-darmstadt.de*

Bernhard A. Schmitt

*Philipps-Universität Marburg, Department of Mathematics,
Hans-Meerwein-Straße 6, 35043 Marburg, Germany
schmitt@mathematik.uni-marburg.de*

April 23, 2024

Abstract

This paper is concerned with the theory, construction and application of implicit Peer two-step methods that are super-convergent for variable stepsizes, i.e., preserve their classical order achieved for uniform stepsizes when applied to ODE constrained optimal control problems in a first-discretize-then-optimize setting. We upgrade our former implicit two-step Peer triplets constructed in [Algorithms, 15:310, 2022] to get ready for dynamical systems with varying time scales without losing efficiency. Peer triplets consist of a standard Peer method for interior time steps supplemented by matching methods for the starting and end steps. A decisive advantage of Peer methods is their absence of order reduction since they use stages of the same high stage order. The consistency analysis of variable-stepsize implicit Peer methods results in additional order conditions and severe new difficulties for uniform zero-stability, which intensifies the demands on the Peer triplet. Further, we discuss the construction of 4-stage methods with order pairs (4,3) and (3,3) for state and adjoint variables in detail and provide four Peer triplets of practical interest. We rigorously prove convergence of order $s - 1$ for s -stage Peer methods applied on grids with bounded or smoothly changing stepsize ratios. Numerical tests show the expected order of convergence for the new variable-stepsize Peer triplets.

Key words. Implicit Peer two-step methods, nonlinear optimal control, first-discretize-then-optimize, discrete adjoints, variable stepsizes, super-convergence

1 Introduction

Recently, we have developed and tested third- and fourth-order implicit Peer two-step methods [11, 12, 13] to solve ODE constrained optimal control problems of the form

$$\text{minimize } C(y(T)) \tag{1}$$

$$\text{subject to } y'(t) = f(y(t), u(t)), \quad u(t) \in U_{ad}, \quad t \in (0, T], \tag{2}$$

$$y(0) = y_0, \tag{3}$$

with the state $y(t) \in \mathbb{R}^m$, the control $u(t) \in \mathbb{R}^d$, $f : \mathbb{R}^m \times \mathbb{R}^d \mapsto \mathbb{R}^m$, the objective function $C : \mathbb{R}^m \mapsto \mathbb{R}$, where the set of admissible controls $U_{ad} \subset \mathbb{R}^d$ is closed and convex. The design of efficient time integrators for the numerical solution of such problems with large m arising from semi-discretized time-dependent partial differential equations is still of great interest since difficulties arise through additional adjoint order conditions, some recent literature is [1, 2]. Implicit Peer two-step methods overcome the structural disadvantages of one-step and multi-step methods such as symplectic or generalized partitioned Runge-Kutta methods [6, 9, 14] and backward differentiation formulas [4]. They avoid order reduction of one-step methods, e.g., for boundary control problems of PDEs [13], and have good stability properties. Peer methods also allow the approximation of adjoints in a first-discretize-then-optimize (FDTO) approach with higher order which still seems to be an unsolved problem for multi-step methods. FDTO is the most commonly used method and possesses the advantage of providing consistent gradients for state-of-the-art optimization algorithms. We refer the reader to the detailed discussions in our previous papers [11, 12, 13].

So far we have considered the use of constant stepsizes to approximate the ODE system (2). However, dynamical systems with sub-processes evolving on many different time scales are ubiquitous in applications. Their efficient solution is greatly enhanced by automatic time step variation. A popular strategy is to focus on adaptively optimizing time grids in accordance with local error control, i.e., errors made within a single integration step. However, in optimal control algorithm, the approximation property of adjoint variables and controls heavily depend on the global state errors at any discrete time point. Ideally, higher-order time integrators should not suffer from order reduction when they are applied with smoothly varying stepsizes. Since the optimal control problem requires the solution of a boundary value problem, where solutions from the whole grid have to be saved, higher order methods and adaptive grids may lead to considerable savings in memory. So this paper is concerned with the theory, construction and application of implicit Peer two-step methods that are super-convergent for variable stepsizes, i.e., preserve their classical order achieved for uniform stepsizes. In fact, we are considering triplets of methods where some common standard Peer method is accompanied by different start and end methods satisfying appropriate matching conditions.

Introducing for any $u \in U_{ad}$ the normal cone mapping

$$N_U(u) = \{w \in \mathbb{R}^d : w^T(v - u) \leq 0 \text{ for all } v \in U_{ad}\}, \tag{4}$$

the first-order Karush–Kuhn–Tucker (KKT) optimality conditions read [7, 19]

$$y'(t) = f(y(t), u(t)), \quad t \in (0, T], \quad y(0) = y_0, \tag{5}$$

$$p'(t) = -\nabla_y f(y(t), u(t))^T p(t), \quad t \in [0, T], \quad p(T) = \nabla_y \mathcal{C}(y(T))^T, \tag{6}$$

$$-\nabla_u f(y(t), u(t))^T p(t) \in N_U(u(t)), \quad t \in [0, T]. \tag{7}$$

Throughout the paper, we will make the following two assumptions: (i) There exists a local solution (y^*, u^*, p^*) of the KKT system and (ii) the control uniqueness property as stated in [7] is valid, i.e., for any (y, p) sufficiently close to (y^*, p^*) , there exists a locally unique minimizer $u = u(y, p)$ of the Hamiltonian $H(y, u, p) := p^\top f(y, u)$ over all $u \in U_{ad}$. Then the control $u(t)$ can be explicitly eliminated, yielding the reduced boundary value problem

$$y'(t) = g(y(t), p(t)), \quad y(0) = y_0, \quad (8)$$

$$p'(t) = \phi(y(t), p(t)), \quad p(T) = \nabla_y C(y(T))^\top, \quad (9)$$

with the source functions defined by

$$g(y, p) := f(y, u(y, p)), \quad \phi(y, p) := -\nabla_y f(y, u(y, p))^\top p. \quad (10)$$

This boundary value problem is used in our consistency and convergence analysis.

The paper is organised as follows. In Chapter 2, we derive the discrete system of Karush-Kuhn-Tucker conditions for Peer triplets and reformulate it as boundary value problem with eliminated control. A consistency analysis for the standard and the boundary methods is presented in Chapter 3. Uniform zero-stability is established by enforcing boundedness of matrix families in Chapter 4. In Chapter 5, we will design new 4-stage Peer triplets of practical interest. Convergence for variable stepsizes is studied in Chapter 6. We discuss the results of two optimal control problems in Chapter 7 and conclude with a summary in Chapter 8.

2 Implicit Peer two-step methods with variable stepsizes

We follow the *first-discretize-and-then-optimize* approach. In every time step from t_n to $t_{n+1} := t_n + h_n$, two-step Peer methods use s stages $Y_{ni} \cong y(t_{ni})$, $i = 1, \dots, s$, as solution approximations at off-step points $t_{ni} = t_n + h_n c_i$, $i = 1, \dots, s$, based on a fixed set of nodes which may be considered as elements of a node vector $\mathbf{c} = (c_1, \dots, c_s)$. For ease of writing, also the stages are collected in a large vector, e.g., $Y_n = (Y_{ni})_{i=1}^s$. For variable stepsizes, the two-step structure of the Peer methods requires that some of its coefficients have to change between steps. Hence, we associate with every time step $t_n \rightarrow t_{n+1}$ of the Peer methods given in a redundant formulation by

$$A_n Y_n = B_n Y_{n-1} + h_n K_n F(Y_n, U_n), \quad n = 1, \dots, N, \quad (11)$$

for the approximation of (2), an individual set of three coefficient matrices (A_n, B_n, K_n) . Here, $F(Y_n, U_n) = (f(Y_{ni}, U_{ni}))_{i=1}^s$. As in (11), we will use for a simple matrix like $A_n \in \mathbb{R}^{s \times s}$ and for its Kronecker product $A_n \otimes I_m$ with the identity matrix the same symbol. For the stage approximations Y_0 of the first interval, a one-step method of Runge-Kutta type

$$A_0 Y_0 = a \otimes y_0 + h_0 K_0 F(Y_0, U_0), \quad (12)$$

with $a \in \mathbb{R}^s$ is considered. We allow for a general linear combination for the solution at the end point

$$y_h(T) := \sum_{j=1}^s w_j Y_{nj} = (w^\top \otimes I_m) Y_N, \quad (13)$$

in order to avoid the necessity of choosing $c_s = 1$. The matrices A_n are assumed to be nonsingular. For reasons of computational efficiency, lower triangular matrices A_n and diagonal matrices K_n will be used with the exception of the boundary steps $n = 0, N$.

Considering the discrete Lagrange function

$$\begin{aligned} L(Y, U, P) = & C(y_h(T)) - P_0^\top (A_0 Y_0 - a \otimes y_0 - h_0 K_0 F(Y_0, U_0)) \\ & - \sum_{n=1}^N P_n^\top (A_n Y_n - B_n Y_{n-1} - h_n K_n F(Y_n, U_n)) \end{aligned} \quad (14)$$

with multipliers $P_n \in \mathbb{R}^{ms}$, the additional discrete KKT conditions read, see [12],

$$A_n^\top P_n = B_{n+1}^\top P_{n+1} + h_n \nabla_Y F(Y_n, U_n)^\top K_n^\top P_n, \quad 0 \leq n \leq N-1, \quad (15)$$

$$A_N^\top P_N = w \otimes p_h(T) + h_N \nabla_Y F(Y_N, U_N)^\top K_N^\top P_N, \quad n = N, \quad (16)$$

$$- \nabla_U F(Y_n, U_n)^\top K_n^\top P_n \in N_{U^*}(U_n), \quad 0 \leq n \leq N, \quad (17)$$

where $p_h(T) = \nabla_y C(y_h(T))^\top$ and

$$N_{U^*}(u) = \{w \in \mathbb{R}^{sd} : w^\top (v - u) \leq 0 \text{ for all } v \in U_{ad}^s \subset \mathbb{R}^{sd}\}.$$

Hence, the KKT conditions constitute a discrete boundary value problem for (Y, U, P) described by the 5 equations (11), (12), (15), (16), (17). We note that the forward step (11) and the adjoint step (15) may be simplified, e.g., by multiplication with A_n^{-1} or $A_n^{-\top}$, respectively. However, these changes lead to different „simplified“ coefficients. Hence, the redundant formulation of the standard method with 3 matrices (A_n, B_n, K_k) adds degrees of freedom required for the additional order conditions, [11].

Eliminating the discrete controls $U_n = U_n(Y_n, P_n)$ by the control uniqueness property and defining

$$\Phi(Y_n, K_n^\top P_n) := (\phi(Y_{ni}, (K_n^\top P_n)_i))_{i=1}^s, \quad G(Y_n, P_n) := (g(Y_{ni}, P_{ni}))_{i=1}^s, \quad (18)$$

the discrete boundary value problem reads in compact form,

$$A_0 Y_0 = a \otimes y_0 + h_0 K_0 G(Y_0, P_0), \quad (19)$$

$$A_n Y_n = B_n Y_{n-1} + h_n K_n G(Y_n, P_n), \quad 1 \leq n \leq N, \quad (20)$$

$$y_h(T) = (w^\top \otimes I_m) Y_N, \quad (21)$$

$$A_n^\top P_n = B_{n+1}^\top P_{n+1} - h_n \Phi(Y_n, K_n^\top P_n), \quad 0 \leq n \leq N-1, \quad (22)$$

$$A_N^\top P_N = w \otimes \nabla_y C(y_h(T))^\top - h_N \Phi(Y_N, K_N^\top P_N), \quad n = N. \quad (23)$$

We will now study the consistency of the overall scheme.

3 Consistency

3.1 Order conditions for the inner grid

Since we are interested in localized error estimates taking account of nodes outside the standard interval $[0, 1]$, i.e. with $c^* := \max\{c_1, \dots, c_s, 1\} \geq 1$, we consider the whole interval $[0, T]$ as part of

the union $\bigcup_{n=0}^N \pi_n \subset [0, T^*]$ of subintervals $\pi_n := [t_n, t_n + h_n c^*]$. The order conditions from earlier papers [11, 12] have to be extended now with the aid of the scaling matrix $S_{n,r} = \text{diag}_i(\sigma_n^{i-1}) \in \mathbb{R}^{r \times r}$, $1 \leq r \leq s$, depending on the local stepsize ratio $\sigma_n = h_n/h_{n-1} > 0$, $n \geq 1$, which will be restricted by lower and upper bounds later on. In principle, we will again consider conditions with two orders $r, q \leq s$ applied uniformly for all $\sigma \in \mathbb{R}$, where r denotes the local order of the standard scheme (11) and q the local order for the adjoint scheme (15). For the forward step (11), such conditions have already been presented in, e.g. [17]. They will be given in (26). Hence we derive in detail only the order conditions for the adjoint step (15) with a diagonal matrix K_n . Using Taylor expansion at t_n for $t_{nj} = t_n + h_n c_j$ and $t_{n+1} + h_{n+1} c_j = t_n + h_n(1 + \sigma_{n+1} c_j)$, this step has the following residuals τ_n^P if it is used with values $y(t_{ni}), p(t_{ni})$ and $\nabla_y f(y(t_{ni}), u(t_{ni}))^\top p(t_{ni}) = -p'(t_{ni})$. Let $A_n := (a_{ij})_{i,j=1}^s$, $B_n := (b_{ij})_{i,j=1}^s$ and $K_n = \text{diag}(\kappa_{jj})_{j=1}^s$. With $z_n := h_n d/dt$ and $\exp_q(z) = \sum_{j=0}^{q-1} z^j/j!$, we then obtain for the local error the expression

$$\begin{aligned} A_n^\top \tau_n^P &:= \left(\sum_{i=1}^s (a_{ij} p(t_{ni}) - b_{ij} p(t_{n+1,i})) + h_n \kappa_{jj} p'(t_{nj}) \right)_{j=1}^s \\ &= \left(A_n^\top \exp_q(\mathbf{c} z_n) - B_n^\top \exp_q((\mathbb{1} + \sigma_{n+1} \mathbf{c}) z_n) + z_n K_n \exp_{q-1}(\mathbf{c} z_n) \right) p|_{t_n} + O(z_n^q p). \end{aligned} \quad (24)$$

We introduce the powers of the node vector $\mathbf{c}^k = (c_1^k, \dots, c_s^k)^\top$, the Vandermonde matrices $V_q = (\mathbb{1}, \mathbf{c}, \dots, \mathbf{c}^{q-1}) \in \mathbb{R}^{s \times q}$, the Pascal matrix $\mathcal{P}_q = ((j-1)!) \in \mathbb{R}^{q \times q}$ and the nilpotent matrix $\tilde{E}_q = (i\delta_{i+1,j}) \in \mathbb{R}^{q \times q}$ commuting with $\mathcal{P}_q = \exp(\tilde{E}_q)$. Then, with the identity

$$((1 + \sigma c_i)^{k-1})_{i,k=1}^{s,q} = \sum_{l=1}^k c_i^{l-1} \sigma^{l-1} \binom{k-1}{l-1} = V_q S_q(\sigma) \mathcal{P}_q,$$

the conditions for adjoint local order $q \leq s$ may be deduced from (24) and combined in matrix form to

$$A_n^\top V_q = B_{n+1}^\top V_q S_{n+1,q} \mathcal{P}_q - K_n V_q \tilde{E}_q. \quad (25)$$

Transposing equation (25), we may present the conditions for local order $r \leq s$ of the forward method and local order $q \leq s$ of the adjoint method together as

$$A_n V_r = B_n V_r \mathcal{P}_r^{-1} S_{n,r}^{-1} + K_n V_r \tilde{E}_r, \quad (26)$$

$$V_q^\top A_n = \mathcal{P}_q^\top S_{n+1,q} V_q^\top B_{n+1} - \tilde{E}_q^\top V_q^\top K_n. \quad (27)$$

The equations of lowest order, often called preconsistency conditions will be used frequently and are repeated here for easier reference,

$$A_n \mathbb{1} = B_n \mathbb{1}, \quad \mathbb{1}^\top A_n = \mathbb{1}^\top B_{n+1}. \quad (28)$$

Also for later reference, we note the precise form of the local error resulting from these order conditions. Since the adjoint step analyzed in (24) uses nodes in $\pi_n \cup \pi_{n+1}$, $n < N$, and the forward step from $\pi_{n-1} \cup \pi_n$, we introduce the following short-hand notation for the norms used in the remainder terms. For $v \in C[0, T^*]$ let

$$\|v\|_{[n]} := \max\{\|v(x)\| : x \in \pi_{n-1} \cup \pi_n \cup \pi_{n+1}\}, \quad 0 \leq n \leq N, \quad (29)$$

with the agreement that $\pi_0 = \pi_{N+1} = \emptyset$. Now, if (26), (27) hold and $y, p \in C^{k+1}[0, T^*]$ for $k \leq r$ resp. $k \leq q$, then the local errors satisfy

$$\tau_n^Y = h_n^k \beta_k(\sigma_n) y^{(k)}(t_n) + O(h_n^{k+1} \|y^{(k+1)}\|_{[n]}), \quad (30)$$

$$\beta_k(\sigma) := \frac{1}{k!} A_n^{-1} (A_n \mathbf{c}^k - B_n (\mathbf{c} - \mathbb{1})^k \sigma^{-k} - k K_n \mathbf{c}^{k-1}),$$

$$\tau_n^P = h_n^k \beta_k^\dagger(\sigma_{n+1}) p^{(k)}(t_n) + O(h_n^{k+1} \|p^{(k+1)}\|_{[n]}), \quad (31)$$

$$\beta_k^\dagger(\sigma) := \frac{1}{k!} A_n^{-\top} (A_n^\top \mathbf{c}^k - B_{n+1}^\top (\mathbb{1} + \sigma \mathbf{c})^k + k K_n \mathbf{c}^{k-1}). \quad (32)$$

Using the current stepsize h_n also in the remainder is justified since stepsizes will be restricted to some interval $\sigma_n \in [\underline{\sigma}, \bar{\sigma}]$ on the positive axis, for instance with $\underline{\sigma} = 1/\bar{\sigma} < 1$. Of course, only the remainder terms appear here for $k < r$ resp. $k < q$.

Before proceeding, we like to recall our basic design strategy from [12] for matching order conditions for the three parts of the Peer triplets. Since the boundary steps (12) and (16) are applied once only, they contribute to the global error with their local order. For the time steps of the inner grid, we will prevent the usual loss of one order from the local to the global error by exploiting again a super-convergence property. Accordingly, all steps forward in time have to satisfy conditions with the same local order $r < s$ and the adjoint steps for order $q < s$ for arbitrary stepsize ratios σ_n .

Obviously, the two boundary steps (12), (16) have one-step character and a triangular form of, e.g., A_0, K_0 would limit the (local) stage order to two. Hence, we have to consider coefficient matrices A_n, K_n , $n = 0, N$, of more general form for the two boundary methods. Of course, the loss of triangularity increases the computational expense by much. However, this affects only the boundary steps which present only a very small part of the full boundary value problem. In the boundary steps, $n = 0, N$, one additional *one-leg-condition*

$$(\mathbf{c}^{q_b-1})^\top K_n = \mathbb{1}^\top K_n C^{q_b-1}, \quad C := \text{diag}(c_1, \dots, c_s), \quad (33)$$

applies with order $q_b = q - 1$, which is nontrivial for $q = 3$, see (61) in [12]. It is obviously satisfied with any $q_b \in \mathbb{N}$ for diagonal matrices K_n like those from the rest of the grid.

3.2 Step-independent matrices A, K in the standard method

Using different coefficients in every time step would mean a tremendous overhead for the implementation of such methods. Instead, we will use exceptional coefficients in the boundary steps only and use fixed coefficients $A_n \equiv A$, $K_n \equiv K$ of our *standard method* in the inner time steps with $1 \leq n < N$. There, only B_n may change with n . In fact, the order conditions will show that it will depend on the stepsize ratio σ_n only: $B_n = B(\sigma_n)$, $n = 1, \dots, N$, with a certain matrix function $B(\sigma)$ depending on the parameter $\sigma \in \mathbb{R}$. This strategy has been used earlier, e.g. [17], but now it has far reaching consequences on the structure of all three coefficient matrices $A, B(\sigma), K$.

Since now 2 of the 3 matrices in the order conditions (26) are independent of σ_n , the same holds for the third one containing $B(\sigma_n)$, which means that

$$AV_r - KV_r \tilde{E}_r = B(\sigma_n) V_r \mathcal{P}_r^{-1} S_{n,r}^{-1} \equiv B(1) V_r \mathcal{P}_r^{-1}, \quad (34)$$

since $S_{n,r} = I_r$ for $\sigma_n = 1$. Hence, A and K may be dropped in the present discussion. The same argument for condition (27) means that also

$$\mathcal{P}_q^{-\top} (V_q^\top A + \tilde{E}_q^\top V_q^\top K) = S_{n,q} V_q^\top B(\sigma_n) \equiv V_q^\top B(1) \quad (35)$$

is independent of σ_n . Combining both conditions fixes large parts of the matrix function $B(\sigma)$ and as a consequence also of A and K . We note that the matrix $\mathcal{Q}_{q,r}$ appearing in the next lemma plays a fundamental role in the matching conditions for the three methods constituting the triplet, see also [12].

It is obvious that due to the redundant formulation of the standard Peer method with three matrices (A, B_n, K) any nontrivial multiple of it also satisfies the order conditions. In order to eliminate unnecessary degrees of freedom from the upcoming discussion which will disappear later on we assume the following normalization:

$$\mathbb{1}^\top A \mathbb{1} = 1, \quad (36)$$

which will naturally come up through the order conditions for the boundary steps.

Lemma 3.1 *Let the order conditions (26) and (27) be satisfied with $1 \leq q, r \leq s$ for two different stepsize ratios σ_n , at least, and assume (36). Then the matrix $\mathcal{Q}_{q,r}(\sigma) := V_q^\top B(\sigma) V_r \mathcal{P}_r^{-1}$ satisfies*

$$\mathcal{Q}_{q,r}(\sigma) = e_1 e_1^\top \in \mathbb{R}^{q \times r} \quad (37)$$

and is independent of σ .

Proof: By (28) the assumption (36) leads to $1 = \mathbb{1}^\top A \mathbb{1} = \mathbb{1}^\top B(\sigma) \mathbb{1} = e_1^\top \mathcal{Q}_{q,r}(\sigma) e_1$. Multiplying (34) by V_q^\top from the left and (35) by $V_r \mathcal{P}_r^{-1}$ from the right yields

$$\begin{aligned} V_q^\top B(\sigma_n) V_r \mathcal{P}_r^{-1} S_{n,r}^{-1} = \mathcal{Q}_{q,r}(1) &\iff \mathcal{Q}_{q,r}(\sigma_n) = \mathcal{Q}_{q,r}(1) S_{n,r}, \\ S_{n,q} \mathcal{Q}_{q,r}(\sigma_n) = \mathcal{Q}_{q,r}(1) &\Rightarrow \mathcal{Q}_{q,r}(1) = S_{n,q} \mathcal{Q}_{q,r}(\sigma_n) = S_{n,q} \mathcal{Q}_{q,r}(1) S_{n,r}, \end{aligned}$$

where the identity from the first line was inserted in the last step. Hence the elements of $\mathcal{Q}_{q,r}(1) = (\gamma_{ij})$ satisfy $\gamma_{ij}(1 - \sigma_n^{i+j-2}) = 0$ for $i \leq q, j \leq r$. Fulfilling this condition for two different values of σ_n leaves as only solution the one from assertion (37) since $\gamma_{11} = 1$. \square

This Lemma is the first place showing that matrices congruent to the original coefficients $A, B(\sigma), K$ may have a very restricted form. Since these matrices will be discussed frequently, we introduce a shorthand notation for them and their submatrices:

$$\hat{A}_{q,r} := V_q^\top A V_r, \quad \hat{B}_{q,r}(\sigma) := V_q^\top B(\sigma) V_r, \quad \hat{K}_{q,r} := V_q^\top K V_r, \quad (38)$$

and missing subscripts indicate the matrices of full dimension $s \times s$. This notation also simplifies the generalized formulation of combined order conditions discussed in [12]. Multiplying (26) by V_q^\top from the left and condition (27) with a shifted index $n+1 \rightarrow n$ by V_r from the right yields the necessary conditions

$$\hat{A}_{q,r} = \hat{B}_{q,r}(\sigma) \mathcal{P}_r^{-1} S_{n,r}^{-1} + \hat{K}_{q,r} \tilde{E}_r, \quad (39)$$

$$\hat{A}_{q,r} = \mathcal{P}_q^\top S_{n,q} \hat{B}_{q,r}(\sigma) - \tilde{E}_q^\top \hat{K}_{q,r}. \quad (40)$$

Obviously, $\hat{A}_{q,r}$ may be eliminated yielding the combined necessary condition

$$\begin{aligned} \hat{K}_{q,r} \tilde{E}_r + \tilde{E}_q^\top \hat{K}_{q,r} &= \mathcal{P}_q^\top S_{n,q} \hat{B}_{q,r}(\sigma) - \hat{B}_{q,r}(\sigma) \mathcal{P}_r^{-1} S_{n,r}^{-1} \\ &= \mathcal{P}_q^\top S_{n,q} \mathcal{Q}_{q,r}(\sigma) \mathcal{P}_r - \mathcal{Q}_{q,r}(\sigma) S_{n,r}^{-1} = \mathbb{1}_q \mathbb{1}_r^\top - e_1 e_1^\top \in \mathbb{R}^{q \times r}, \end{aligned} \quad (41)$$

by Lemma 3.1 and since $\mathbb{1}^\top \mathcal{P}_k = \mathbb{1}_k^\top$. We note that the map

$$\mathcal{L}_{q,r} : X \mapsto X \tilde{E}_r + \tilde{E}_q^\top X \quad (42)$$

on the left-hand side of (41) is singular, and $e_1^\top \mathcal{L}_{q,r}(X)e_1 = 0$ for any X . For a more detailed discussion see [12, 15]. We like to point out that (37) and (41) refer to orders r, q used with σ -uniform order conditions. The strong restriction (37) for \mathcal{Q} will limit these orders to $q, r \leq s-1$ for sufficiently stable methods. However, for $r = s-1$ we will try later on to improve the accuracy by applying additional order conditions of order $r_1 = s$ for $\sigma = 1$ only.

Lemma 3.1 not only restricts the form of $\hat{B}(\sigma)$ to a large extent, it also leaves only a few free parameters in the σ -independent matrices A and K .

Corollary 3.1 *Under the assumptions of Lemma 3.1 the coefficient matrices of the standard Peer method satisfy*

$$\hat{B}_{q,r}(\sigma) = V_q^\top B(\sigma) V_r = e_1 \mathbb{1}^\top \in \mathbb{R}^{q \times r}, \quad \hat{A}_{q,r} = V_q^\top A V_r = \left(\frac{j-1}{i+j-2} \right)_{i,j} \in \mathbb{R}^{q \times r}, \quad (43)$$

with $e_1^\top \hat{A} e_1 = \mathbb{1}^\top A \mathbb{1} = 1$. The matrix $\hat{K} = V_s^\top K V_s$ has Hankel form equaling the Hilbert matrix in its first $q+r-2$ antidiagonals.

Proof: Multiplying (37) by \mathcal{P}_r from the right yields the assertion for $V_q^\top B(\sigma) V_r$ since $e_1^\top \mathcal{P}_r = \mathbb{1}_r^\top$. Since the matrix K is diagonal, the matrix $\hat{K} = (\hat{\kappa}_{ij}) := V_s^\top K V_s$ and all its submatrices possess Hankel form, $\hat{\kappa}_{ij} = \xi_{i+j-1}$, $1 \leq i, j \leq s$. Hence, equation (41) is satisfied as $0 = 0$ for $i = j = 1$ and means

$$\hat{\kappa}_{i,j-1}(j-1) + (i-1)\hat{\kappa}_{i-1,j} = (i+j-2)\xi_{i+j-2} = 1 \quad (44)$$

for $3 \leq i+j \leq q+r$. Non-existent elements of \hat{K} with index zero are canceled by vanishing factors. Setting $\ell := i+j-2 \geq 1$, we obtain $\xi_\ell = 1/\ell$ for $1 \leq \ell \leq q+r-2$.

Now, equation (39) shows that $\hat{A}_{q,r} = \mathcal{Q}_{q,r} S_{n,r}^{-1}(\sigma) + \hat{K}_{q,r} \tilde{E}_r = e_1 e_1^\top + \hat{K}_{q,r} \tilde{E}_r$, where \tilde{E}_r shifts columns of $\hat{K}_{q,r}$ to the right by one. Hence, the element from the latest anti-diagonal of $\hat{K}_{q,r}$ entering $\hat{A}_{q,r}$ is $\hat{\kappa}_{q,r-1} = \xi_{q+r-2} = 1/(q+r-2)$ still belonging to the Hilbert part. Hence, the formula (43) follows where the first element of $\hat{A}_{q,r}$ also fits in by setting $0/0 = 1$, here. \square

Remark 3.1 *The Corollary shows that the diagonal elements of the matrix $K = \text{diag}_i(\kappa_{ii})$ are weights of a quadrature formula associated with the nodes c_i , since*

$$\hat{\kappa}_{ij} = \sum_{\ell=1}^s \kappa_{\ell\ell} c_\ell^{i+j-2} = \frac{1}{i+j-1} = \int_0^1 t^{i+j-2} dt, \quad 2 \leq i+j \leq q+r. \quad (45)$$

Hence, the matrix K is uniquely determined by the nodes for $q+r \geq s+1$. And if K has only positive diagonal elements it induces a positive quadrature formula where the node polynomial is an orthogonal polynomial for some appropriate weight function, [20].

The design of the standard method will be based on the hat-matrices (43) since the Corollary leaves few free parameters only in their entries. However, the matrix A from the standard method has to satisfy a second restriction on its structure since an efficient implementation of the time step requires triangular form of A . This restriction corresponds to a set of $s(s-1)/2$ conditions

(6 for $s = 4$) which have to be solved with the aid of the remaining parameters in \hat{A} and the Vandermonde matrix V . With local orders $q = r = s - 1$ of the methods the remaining $2s - 1$ free parameters (7 for $s = 4$) in \hat{A} may seem to be sufficient for this task without restricting the nodes c_i . Unfortunately, this is not fully true for $s \geq 4$ since linear dependencies lead to some algebraic restrictions on the nodes c_i , whose number increases with larger stage numbers s .

Lemma 3.2 *The s -stage standard method $(A, B(\sigma), K)$ with lower triangular matrix A can satisfy the order conditions (26), (27) with $q = r = s - 1$ for different stepsize ratios σ_n only if the nodes c_1, \dots, c_s satisfy a set of $(s - 2)(s - 3)/2$ algebraic equations.*

Proof: Knowing that $\hat{A}_{r,r} = V_r^\top A V_r$ has fixed entries given by (43), for $r = s - 1$ we consider the square Vandermonde matrix $\bar{V}_r \in \mathbb{R}^{r \times r}$ without the last node c_s . Thus, we may write $V_r^\top = \bar{V}_r^\top (I_r, v)$ with $v^\top = (1, c_s, \dots, c_s^r) \bar{V}_r^{-1}$. Splitting the lower triangular matrix A in the same way, the definition of $\hat{A}_{r,r}$ is equivalent with

$$\bar{V}_r^{-\top} \hat{A}_{r,r} \bar{V}_r^{-1} = (I_r, v) \begin{pmatrix} \bar{A} & 0 \\ a_s^\top & a_{ss} \end{pmatrix} \begin{pmatrix} I \\ v^\top \end{pmatrix} = \bar{A} + v(a_s^\top + a_{ss}v^\top).$$

Since the leading block \bar{A} is also lower triangular, contributions from A above the main diagonal come through the vector $a_s^\top + a_{ss}v^\top$ only. Considering now the first $r - 1$ entries of the last column number r in this identity, we obtain the linear equation

$$(\bar{V}_r^{-\top} \hat{A}_{r,r} \bar{V}_r^{-1} e_r)_{1 \dots r-1} = \alpha_r \cdot v_{1 \dots r-1}$$

containing one single parameter $\alpha_r := a_{sr} + a_{ss}v^\top e_r$ from \hat{A} only. Solutions α_r do only exist if the vectors on both sides are linearly dependent which corresponds to the vanishing of $r - 2$ determinants of size 2×2 . This argument repeats for the other columns with shrinking vector length until column number 3 with one 2×2 -determinant. This means, one condition for $s = 4$, two more for $s = 5$, etc. \square

The Lemma shows that Peer methods with orders $r = q = s - 1$ for variable stepsizes probably do not exist for $s \geq 6$ since the number of restrictions on the s nodes is six for $s = 6$ and three for $s = 5$.

3.3 Boundary methods

In addition to the standard method $(A, B(\sigma), K)$ used in the time steps with $1 \leq n < N$, exceptional methods for the start ($n = 0$) and the final step ($n = N$) will be used in order to gain more flexibility in the accurate approximation of the boundary conditions. And as mentioned before local order higher than two is not possible with triangular coefficients A_0, A_N, K_0, K_N . The order conditions for the starting method (12) are

$$A_0 V_r = a e_1^\top + K_0 V_r \tilde{E}_r, \quad (46)$$

$$V_q^\top A_0 + \tilde{E}_q^\top V_q^\top K_0 = \mathcal{P}_q^\top S_{1,q} V_q^\top B(\sigma_1) = V_q^\top A + \tilde{E}_q^\top V_q^\top K, \quad (47)$$

where the forward condition is copied from [11] and the adjoint condition uses (27) twice with $n = 0$ and $n > 0$. Hence, both conditions are independent of the ratio σ_1 and also A_0, K_0 may be constant.

As a change to earlier papers [11, 12], we will now use the matrix $B(\sigma)$ from the standard method also in the end step $n = N$. Hence, for the end method, the forward condition (34) is complemented with only one adjoint condition yielding

$$A_N V_r - K_N V_r \tilde{E}_r = B(1) V_r \mathcal{P}_r^{-1}, \quad (48)$$

$$A_N^\top V_q + K_N^\top V_q \tilde{E}_q = w \mathbb{1}^\top, \quad (49)$$

where the first condition uses (34) and second condition comes from [11]. Since $\tilde{E}_r e_1 = 0$, first consequences of (46), (49) are

$$a = A_0 \mathbb{1}, \quad w = A_N^\top \mathbb{1}. \quad (50)$$

Order r of accuracy for the extrapolation step (13) also requires that, see [12],

$$w^\top V_r = \mathbb{1}_r^\top. \quad (51)$$

Comparing with (50), this means that $\mathbb{1}^\top A_N V_r = e_1^\top V_s^\top A V_r = \mathbb{1}_r^\top$ and hence the r first entires of \hat{A}_N coincide with those from \hat{A} , see (43).

Similar to (41), the order conditions for each boundary method can be combined to the following necessary conditions. They are much simpler now than those in [12] due to Lemma 3.1 which showed that $\mathcal{Q}_{q,r} = e_1 e_1^\top$. These combined conditions are

$$\mathcal{L}_{q,r}(V_q^\top K_0 V_r) = \mathcal{P}_q^\top \mathcal{Q}_{q,r} \mathcal{P}_r - V_q^\top a e_1^\top = \mathbb{1} \mathbb{1}^\top - V_q^\top a e_1^\top, \quad (52)$$

$$\mathcal{L}_{q,r}(V_q^\top K_N V_r) = \mathbb{1} \mathbb{1}^\top - \mathcal{Q}_{q,r} = \mathbb{1} \mathbb{1}^\top - e_1 e_1^\top, \quad (53)$$

with the map $\mathcal{L}_{q,r}$ defined in (42). Here, the singularity of this map with the property $e_1^\top \mathcal{L}_{q,r} e_1 = 0$ requires that $e_1^\top \mathcal{Q}_{q,r} e_1 = 1$ in (53) which was the reason for assuming the normalization (36) above. And in (52) it requires that $1 = e_1^\top V_q^\top a = \mathbb{1}^\top a = \mathbb{1}^\top A_0 \mathbb{1}$.

An additional constraint comes from the one-leg-condition. Rewriting (33) with $q_b = 2$ for \hat{K}_0 , we see that $\mathbf{c}^\top K_0 V_r = e_2^\top V_q^\top K_0 V_r = e_1^\top K_0 C V_r$, where the product $C V_r$ causes a shift in the columns of V_{r+1} to the left. This means that \hat{K}_0 has Hankel form in its first two rows, $\hat{\kappa}_{1,j}^{(0)} = \hat{\kappa}_{2,j-1}^{(0)}$, $j \geq 2$. And similar to (44), this property carries over to $\mathcal{L}_{2,r}(V_2^\top K_0 V_r)$. Hence, (52) has solutions satisfying (33) only if $V_2^\top a = e_1 \in \mathbb{R}^2$, which by (50) means

$$\mathbb{1}^\top A_0 \mathbb{1} = 1, \quad \mathbf{c}^\top A_0 \mathbb{1} = 0. \quad (54)$$

Summing up, the three methods in the Peer triplet use a set of seven coefficient matrices (A_0, K_0) , $(A, B(\sigma), K)$, $(A_N, B(\sigma_N), K_N)$, where the parameter-dependent matrix $B(\sigma)$ is the same in all time steps. The combined equations (52), (53) allow for a detached design of the standard method $(A, B(\sigma), K)$ without reference to the boundary methods since all necessary restrictions for their existence are known.

4 Boundedness of matrix families

A severe new difficulty arising for variable-stepsize Peer methods is uniform zero-stability which requires that arbitrary long products

$$\bar{B}_n \bar{B}_{n-1} \cdots \bar{B}_k, \quad 0 \leq k \leq n, \quad (55)$$

of stability matrices $\bar{B}_n := A^{-1}B_n = A^{-1}B(\sigma_n)$ are uniformly bounded. We note that the stability matrices of the adjoint steps (15) are related by $A^{-\top}B(\sigma)^\top = (B(\sigma)A^{-1})^\top$. Uniform boundedness of long products is connected with the problem of the *joint spectral radius* of matrix families. However, to our knowledge no general, applicable theory exists for this problem, see, e.g. [5]. Instead, as in [16], we incorporate the construction of a suitable norm satisfying $\|\bar{B}_n\| = 1$ for all interior steps n into the design and search process of the standard peer method.

As a consequence of the conditions (28), the matrix \bar{B}_n possesses the eigenvalue one with known eigenvectors and the super-convergence effect that will be exploited later on requires that one is an isolated dominant eigenvalue whose absolute value exceeds that of all others sufficiently, see (75). Hence, our objective is to construct a constant similarity transformation which separates the eigenvalue one in block diagonal form such that a simple norm of the lower block is uniformly bounded below one for stepsize ratios σ_n from a reasonably large interval $[\underline{\sigma}, \bar{\sigma}] \ni 1$.

A first clue to the construction of such a norm gives Corollary 3.1 which we discuss in detail here for the case of interest with $q = r = 3 < s = 4$. The Corollary shows that

$$\hat{A} = \begin{pmatrix} 1 & 1 & 1 & \hat{a}_{14} \\ 0 & \frac{1}{2} & \frac{2}{3} & \hat{a}_{24} \\ 0 & \frac{1}{3} & \frac{1}{2} & \hat{a}_{34} \\ \hat{a}_{41} & \hat{a}_{42} & \hat{a}_{43} & \hat{a}_{44} \end{pmatrix}, \quad \hat{B}(\sigma) = \begin{pmatrix} 1 & 1 & 1 & \hat{a}_{14} \\ 0 & 0 & 0 & \hat{b}_{24}(\sigma) \\ 0 & 0 & 0 & \hat{b}_{34}(\sigma) \\ \hat{a}_{41} & \hat{b}_{42}(\sigma) & \hat{b}_{43}(\sigma) & \hat{b}_{44}(\sigma) \end{pmatrix}, \quad (56)$$

and $\hat{K} = \text{hankel}(1, \frac{1}{2}, \frac{1}{3}, \frac{1}{4}, \hat{k}_5, \hat{k}_6, \hat{k}_7)$. We confirm that the first rows and columns of \hat{A}, \hat{B} are identical and independent of σ due to (28). The elements in their fourth rows and columns may be subject to further restrictions. Written with these transformed matrices $\hat{A}, \hat{B}, \hat{K}$, the full set of order conditions (26),(27) simplifies. With selection matrices $\hat{I}_k = \begin{pmatrix} I_k \\ 0^\top \end{pmatrix} \in \mathbb{R}^{s \times k}$ it reads

$$\left(\hat{A} - \hat{K}\tilde{E}_s - \hat{B}(\sigma)P_s^{-1}S^{-1} \right) \hat{I}_r = 0, \quad (57)$$

$$\hat{I}_q^\top \left(P_s^{-\top}(\hat{A} + \tilde{E}_s^\top \hat{K}) - S\hat{B}(\sigma) \right) = 0, \quad (58)$$

and may be solved easily for $q, r \geq 3$ by

$$\begin{aligned} \hat{b}_{42} &= \hat{a}_{41} + \sigma\hat{a}_{42} - \frac{1}{4}\sigma, \\ \hat{b}_{43} &= \hat{a}_{41} + \sigma(2\hat{a}_{42} - \frac{1}{2}) + \sigma^2(\hat{a}_{43} - 2\hat{k}_5), \\ \hat{b}_{24} &= \sigma^{-1}\left(\frac{1}{4} - \hat{a}_{14} + \hat{a}_{24}\right), \\ \hat{b}_{34} &= \sigma^{-2}\left(-\frac{1}{2} + \hat{a}_{14} - 2\hat{a}_{24} + \hat{a}_{34} + 2\hat{k}_5\right). \end{aligned} \quad (59)$$

For $q = r = 3$, only the last element $\hat{b}_{44}(\sigma)$ of $\hat{B}(\sigma)$ is an unrestricted parameter. And we remind that other elements except $\hat{a}_{14}, \hat{a}_{41}$ are determined by requiring triangularity of the matrix $A = V^{-\top}\hat{A}V^{-1}$.

The stability matrix $\bar{B}(\sigma) = A^{-1}B(\sigma)$ of the standard method is similar to the matrix

$$\hat{A}^{-1}\hat{B}(\sigma) = V_s^{-1}A^{-1}B(\sigma)V_s = V_s^{-1}\bar{B}(\sigma)V_s, \quad (60)$$

and an analogous result holds for the adjoint stability matrix $(B(\sigma)A^{-1})^\top$. Since the factor L_A in the LU-decomposition $\hat{A} = L_A U_A$ inherits the first column from \hat{A} and U_A its first row, a further

stepsize-independent similarity yields a very simple structure for both stability matrices through

$$\begin{aligned} B_{LU}(\sigma) &:= L_A^{-1} \hat{B}(\sigma) U_A^{-1} = U_A (\hat{A}^{-1} \hat{B}(\sigma)) U_A^{-1} = L_A^{-1} (\hat{B}(\sigma) \hat{A}^{-1}) L_A \\ &= \left(\begin{array}{c|ccc} 1 & 0 & 0 & 0 \\ \hline & B_{se}(\sigma) & & \end{array} \right) = \begin{pmatrix} 1 & 0 & 0 & 0 \\ 0 & 0 & 0 & * \\ 0 & 0 & 0 & * \\ 0 & * & * & * \end{pmatrix} \end{aligned} \quad (61)$$

where the last matrix is a sketch for $s = 4$ and $q = r \geq 3$. Obviously, $B_{LU}(\sigma)$ has block diagonal form separating the dominant eigenvalue one from the rest, where the asterisks represent elements of $B_{se}(\sigma)$ which may be nontrivial. The tailored norm $\|\bar{B}_n\| = 1$ will use the maximum norm for the southeast block $B_{se}(\sigma)$ with an additional scaling.

As in [16], we look for additional scalings with a diagonal matrix $\bar{\Omega} = \text{diag}(\omega_2, \dots, \omega_s)$ such that

$$\|\bar{\Omega}^{-1} B_{se}(\sigma) \bar{\Omega}\|_\infty \leq \tilde{\gamma} < 1, \quad (62)$$

for an appropriate set of stepsize ratios σ . Then, for the positive vector $\bar{\omega} := \bar{\Omega} \mathbf{1} > 0$, the inequality $|B_{se}(\sigma)| \bar{\omega} \leq \tilde{\gamma} \bar{\omega}$ holds and quasi-optimal scalings may be computed efficiently by solving a linear program:

$$\min \mathbf{1}^\top \bar{\omega} : \bar{\omega} \geq \mathbf{1}, \quad (\tilde{\gamma} I - |B_{se}(\sigma)|) \bar{\omega} \geq 0 \quad \text{for all } \sigma \in \mathcal{S}, \quad (63)$$

with a small set of stepsize ratios, e.g., $\mathcal{S} := \{1/\hat{\sigma}, 1, \hat{\sigma}\}$, $\hat{\sigma} > 1$. Since $B_{se}(\sigma)$ is a continuous function, we found that the norm bound $\|\bar{\Omega}^{-1} B_{se}(\sigma) \bar{\Omega}\|_\infty \leq 1$ may hold in rather large σ -intervals $[\underline{\sigma}, \bar{\sigma}] \supseteq \{1/\hat{\sigma}, 1, \hat{\sigma}\}$ by appropriate definitions of the free parameter $\hat{b}_{44}(\sigma)$.

Remark 4.1 *By (59) the element functions in the last row and column of $\hat{B}(\sigma)$ are determined by order conditions. The only exception is its last element which may be chosen freely for $q, r \leq s - 1$ as an arbitrary function $\hat{b}_{ss}(\sigma)$. Now, due to the triangular forms of L_A and U_A the element $\hat{b}_{ss}(\sigma)$ appears in the last element of B_{se} only having the form $b_{ss}^{LU}(\sigma) = b_{ss}^*(\sigma) + \hat{b}_{ss}(\sigma)/u_{ss}$, $u_{ss} = e_s^\top U_A e_s$. The part $b_{ss}^*(\sigma)$ which does not depend on $\hat{b}_{ss}(\sigma)$ is easily computed from L_A, U_A and the rest of \hat{B} . The diagonal element $b_{ss}^{LU}(\sigma)$ is not affected by the weight $\bar{\Omega}$ in the norm $\|\bar{\Omega}^{-1} B_{se}(\sigma) \bar{\Omega}\|_\infty$ and contributes to it in the last entry only as $|b_{ss}^{LU}(\sigma)| = |b_{ss}^*(\sigma) + \hat{b}_{ss}(\sigma)/u_{ss}|$. Now, this term may be canceled exactly by choosing*

$$\hat{b}_{ss}(\sigma) = -u_{ss} b_{ss}^*(\sigma). \quad (64)$$

The computation of the diagonal scaling $\bar{\Omega}$ may then follow up by solving (63). Hence, the transformation (61) allows for an explicit norm-optimal choice of the free parameter function $\hat{b}_{ss}(\sigma)$ in $\hat{B}(\sigma)$. This is helpful in some cases where the matrix norm is the bottleneck. However, the choice of $\hat{b}_{ss}(1)$ also influences $A(\alpha)$ -stability and other criteria which may be more important in other cases.

Summarizing this discussion, we will verify the assumption of uniform zero-stability in the convergence theorem below for each standard method $(A, B(\sigma), K)$ by presenting explicitly some weight matrix $W \in \mathbb{R}^{s \times s}$ and an interval for which holds

$$\|\bar{B}(\sigma)\| := \|W^{-1} \bar{B}(\sigma) W\|_\infty = 1, \quad \sigma \in [\underline{\sigma}, \bar{\sigma}], \quad 0 < \underline{\sigma} < 1 < \bar{\sigma}. \quad (65)$$

Since all involved matrix elements are known with rational numbers or square roots, this property may even be proven rigorously. According to (61), the weight matrix may have the form $W = V_s U_A^{-1} \Omega$ with the extended weight $\Omega = \text{diag}(1, \omega_2, \dots, \omega_s)$. A simple property of this matrix is $W e_1 = \mathbb{1}$. For the methods designed later on, we may approximate other entries of W with simpler rational expressions and present these more usable weight matrices explicitly. Since $W^{-1} \bar{B}(\sigma) W = W^{-1} A^{-1} B(\sigma) W = (AW)^{-1} B(\sigma) A^{-1} (AW)$, a similar norm for the adjoint stability matrix $\tilde{B}(\sigma_n)^\top = (B(\sigma_n) A^{-1})^\top$ is given with the matrix $W^\dagger = (AW)^{-\top}$ satisfying

$$\|\tilde{B}(\sigma)^\top\| := \|(W^\dagger)^{-1} A^{-\top} B(\sigma)^\top W^\dagger\|_1 = 1, \quad \sigma \in [\underline{\sigma}, \bar{\sigma}]. \quad (66)$$

The super-convergence effect which prevents the usual loss of one order between local and global error requires that long products of stability matrices converge to the following rank-1-matrices

$$\bar{B}^\infty = \mathbb{1} \mathbb{1}^\top A, \quad (\tilde{B}^\infty)^\top = \mathbb{1} \mathbb{1}^\top A^\top, \quad (67)$$

i.e. $\bar{B}_n \bar{B}_{n-1} \cdots \bar{B}_k \rightarrow \bar{B}^\infty$ ($n \rightarrow \infty$), and $\tilde{B}_n^\top \cdots \tilde{B}_k^\top \rightarrow (\tilde{B}^\infty)^\top$ ($k \rightarrow \infty$). These limits are composed of the left and right eigenvectors to the dominant eigenvalue which are both known due to (28). And the dominant eigenvalue in (67) is $\mathbb{1}^\top A \mathbb{1} = e_1^\top \hat{A} e_1 = 1$ indeed, see (36). It is essential that the weight matrices W, W^\dagger based on the transformation to block diagonal form (61) are independent of σ_n . Hence, this structure carries over to arbitrarily long products

$$B_{LU}(\sigma_n) \cdots B_{LU}(\sigma_k) = \begin{pmatrix} 1 & 0 \\ 0 & B_{se}(\sigma_n) \cdots B_{se}(\sigma_k) \end{pmatrix}. \quad (68)$$

In fact, super-convergence requires that the lower block in (68) tends to zero for $n - k \rightarrow \infty$ for admissible stepsize ratios $\sigma_n, \dots, \sigma_k$ and that infinite sums of products of B_{se} -matrices are uniformly bounded. If (62) is true for $\sigma \in [\underline{\sigma}, \bar{\sigma}]$, then the following norm estimates hold:

$$\|\bar{B}(\sigma) - \bar{B}^\infty\| = \|W^{-1}(\bar{B}(\sigma) - \bar{B}^\infty)W\|_\infty = \|W^{-1} \bar{B}(\sigma) W - e_1 e_1^\top\|_\infty \leq \tilde{\gamma} < 1, \quad (69)$$

$$\|\tilde{B}(\sigma)^\top - (\tilde{B}^\infty)^\top\| = \|(W^\dagger)^{-1}(\tilde{B}(\sigma)^\top - (\tilde{B}^\infty)^\top)W^\dagger\|_1 = \|(W^\dagger)^{-1} \tilde{B}(\sigma)^\top W^\dagger - e_1 e_1^\top\|_1 \leq \tilde{\gamma}, \quad (70)$$

since $W e_1 = \mathbb{1}$ and $\mathbb{1}^\top A W = e_1^\top \hat{A} U_A^{-1} \bar{\Omega} = e_1^\top$. We note that since \bar{B}^∞ and $(\tilde{B}^\infty)^\top$ share both their dominant invariant subspaces with all matrices \bar{B}_n , resp. \tilde{B}_n^\top (maybe except the boundary steps) these bounds transfer to products, e.g., for $1 \leq n < k < N$,

$$\begin{aligned} \|\tilde{B}(\sigma_n)^\top \cdots \tilde{B}(\sigma_{k-1})^\top - (\tilde{B}^\infty)^\top\| &= \|(\tilde{B}(\sigma_n)^\top - (\tilde{B}^\infty)^\top) \cdots (\tilde{B}(\sigma_{k-1})^\top - (\tilde{B}^\infty)^\top)\| \\ &\leq \tilde{\gamma}^{k-n}. \end{aligned} \quad (71)$$

5 Design of 4-stage Peer triplets for variable stepsizes

Efficient Peer triplets need to satisfy more requirements than the order conditions and stability properties discussed so far. Before starting with the actual construction of methods, we mention a few additional useful properties. Time integration methods usually lose one order between local and global error. This loss may be prevented through some super-convergence effect for the standard method, see [12]. Surprisingly, in our present setting the corresponding additional order conditions are fulfilled automatically for $\sigma = 1$. The lemma refers to the error vectors β_r, β_q^\dagger from (30), (31).

Lemma 5.1 *Let the standard method $(A, B(\sigma), K)$ satisfy the order conditions (26), (27) with $q = r = s - 1$ for two different stepsize ratios σ_n , at least.*

a) *Then, also*

$$r! \mathbf{1}^\top A \beta_r(\sigma) = \mathbf{1}^\top (\mathbf{A} \mathbf{c}^r - B(\sigma)(\mathbf{c} - \mathbf{1})^r \sigma^{-r} - rK \mathbf{c}^{r-1}) = (\hat{a}_{1s} - 1)(1 - \sigma^{-r}), \quad (72)$$

$$q! \mathbf{1}^\top A^\top \beta_q^\dagger(\sigma) = \mathbf{1}^\top (A^\top \mathbf{c}^q - B(\sigma)^\top (\mathbf{1} + \sigma \mathbf{c})^q + qK \mathbf{c}^{q-1}) = \hat{a}_{s1}(1 - \sigma^q), \quad (73)$$

where $(\hat{a}_{ij}) = \hat{A} = V_s^\top A V_s$.

b) *Let the standard method also satisfy $\hat{a}_{1s} = 1$ (i.e. $e_1^\top \hat{A} = \mathbf{1}^\top$) and $\hat{k}_s = 1/s$, then*

$$s! \mathbf{1}^\top A \beta_s(\sigma) = \mathbf{1}^\top (\mathbf{A} \mathbf{c}^s - B(\sigma)(\mathbf{c} - \mathbf{1})^s \sigma^{-s} - sK \mathbf{c}^{s-1}) = (1 - \sigma^{-s})(\mathbf{1}^\top \mathbf{A} \mathbf{c}^s - 1). \quad (74)$$

Proof: a) From Corollary 3.1 and condition (28) we know that $e_1^\top \hat{B}(\sigma) = (1, \dots, 1, \hat{a}_{1s}) = \mathbf{1}^\top + (\hat{a}_{1s} - 1)e_s^\top$ is independent of σ , and $e_1^\top \hat{K} e_{s-1} = 1/(s-1)$. In analogy to (57), we see that the first assertion is equivalent with

$$\begin{aligned} & e_1^\top (\hat{A} e_s - \hat{B}(\sigma) \mathcal{P}_s^{-1} e_s \sigma^{-r} - (s-1) \hat{K} e_{s-1}) \\ &= \hat{a}_{1s} - (\mathbf{1}^\top + (\hat{a}_{1s} - 1)e_s) \mathcal{P}_s^{-1} e_s \sigma^{-r} - 1 = (\hat{a}_{1s} - 1)(1 - \sigma^{-r}), \end{aligned}$$

since $\mathbf{1}^\top \mathcal{P}_s^{-1} = e_1^\top$. Now, the first column of \hat{B} is $\hat{B}(1)e_1 = e_1 + \hat{a}_{s1}e_s$ and rewriting (73) as before we obtain

$$(e_s^\top \hat{A} - e_s^\top \mathcal{P}_s^\top S_s \hat{B}(\sigma) + (s-1)e_{s-1}^\top \hat{K})e_1 = \hat{a}_{s1} - e_s^\top \mathcal{P}_s^\top (e_1 + \sigma^q \hat{a}_{s1} e_s) + 1 = \hat{a}_{s1}(1 - \sigma^q).$$

b) Due to $\mathbf{1}^\top B(\sigma) \equiv \mathbf{1}^\top A$, we have for $r = s$ that

$$\begin{aligned} & \mathbf{1}^\top (\mathbf{A} \mathbf{c}^s - B(\sigma)(\mathbf{c} - \mathbf{1})^s \sigma^{-s} - sK \mathbf{c}^{s-1}) \\ &= (1 - \sigma^{-s}) \mathbf{1}^\top \mathbf{A} \mathbf{c}^s - \sum_{k=0}^{s-1} \binom{s}{k} (-1)^k \mathbf{1}^\top B(\sigma) \mathbf{c}^k \sigma^{-s} - s \hat{k}_{1,s} = (1 - \sigma^{-s})(\mathbf{1}^\top \mathbf{A} \mathbf{c}^s - 1). \end{aligned}$$

The last step used $\mathbf{1}^\top B \mathbf{c}^k = e_1^\top \hat{B} e_{k+1} = e_1^\top \hat{A} e_{k+1} = 1$, $k \leq s-1$. \square

We note that the expression (72) vanishes under the assumptions of part b) and that the assumption $\hat{k}_{1s} = 1/s$ is automatically satisfied for $s \geq 4$ due to Corollary 3.1, where $q + r - 2 = 2s - 4 \geq s$.

The conditions (72), (73) will cancel the leading terms $\bar{B}^\infty \beta_r(1)$, $(\bar{B}^\infty)^\top \beta_q^\dagger(1)$ in the global error. However, it is also required that products of stability matrices like (55) converge to the rank-1-matrix \bar{B}^∞ in (67). The norm bounds (69), (70) ensure this in theory and they will be used to verify an assumption in the main convergence theorem with an upper bound $\tilde{\gamma}$ quite close to one. However, in computational practice, convergence to \bar{B}^∞ has to be fast enough. So, according to [12] a similar bound with a smaller limit will also be enforced, but only for the eigenvalues. The requirement

$$|\lambda_2(A^{-1}B(1))| \leq \gamma < 1 \quad \text{with } \gamma \approx 0.8 \quad (75)$$

for the absolutely second largest eigenvalue works well in practice. The conditions from Lemma 5.1 are inner products with the error vectors canceling only the leading error terms. In order to cover

their full impact, we also monitor the whole error vectors in the design process and introduce

$$err_{r,n} = \frac{1}{r!} \|\mathbf{c}^r - A_n^{-1}B(1)(\mathbf{c} - \mathbf{1})^r - rA_n^{-1}K_n\mathbf{c}^{r-1}\|_\infty, \quad (76)$$

$$err_{q,n}^\dagger = \frac{1}{q!} \|\mathbf{c}^q - A_n^{-\top}B(1)^\top(\mathbf{1} + \mathbf{c})^q + qA_n^{-\top}K_n\mathbf{c}^{q-1}\|_\infty, \quad (77)$$

again as the essential error constants [12]. Modifications are required at the boundaries as

$$err_{r,0} = \frac{1}{r!} \|\mathbf{c}^r - rA_0^{-1}K_0\mathbf{c}^{r-1}\|_\infty, \quad err_{q,N}^\dagger = \frac{1}{q!} \|\mathbf{c}^q + A_N^{-\top}(qK_N^\top\mathbf{c}^{q-1} - w)\|_\infty.$$

For the standard method, $1 \leq n < N$, the additional index n is omitted, as usual. Solving the nonlinear equations (11), (12) requires non-singularity of the re-arranged Jacobians $K_n^{-1}A_n - h_n \nabla_Y F$. In the context of stiff problems an appropriate assumption is that

$$\mu_n := \min_j \operatorname{Re} \lambda_j(K_n^{-1}A_n) > 0, \quad n = 0, \dots, N, \quad (78)$$

for the eigenvalues of $K_n^{-1}A_n$. In the design process of the boundary methods further data are monitored like the size of the norms $\|A_N^{-1}B(1)\|$, $\|A_0^{-\top}B(1)^\top\|$ or K_0, K_N .

Considering the assertions of Lemma 5.1, we see that the choices of the method parameters lead to different consequences in (72), (73). On the one hand, for $\hat{a}_{1s} = 1$ resp. $\hat{a}_{s1} = 0$ the conditions for super-convergence are satisfied for arbitrary stepsize ratios σ_n , i.e. for arbitrary grids. However, for $\hat{a}_{1s} \neq 1$ resp. $\hat{a}_{s1} \neq 0$ both expressions have the form $O(1 - \sigma_n) = O(h_n)$ in the n -th time step if we consider smooth grids satisfying $\sigma_n = 1 + O(h_n)$ only. Hence, different design decisions lead to methods with different properties and scopes of application. In the search process it was observed that very favorable properties of the standard method coincide with the choice $c_4 = 1$ for the forward time step, and to a lesser extent with $c_1 = 0$ for the adjoint step. Higher-order methods of this form have a surprising property which is not obvious in our redundant formulation (11) of the Peer method.

Lemma 5.2 *Let the standard method (A, B, K) satisfy the order conditions (34), (35) σ -uniformly for $r = q = s - 1$.*

a) *If also $e_1^\top \hat{A} = \mathbf{1}^\top$ and $c_s = 1$ hold, then*

$$\mathbf{1}^\top A = e_s^\top, \quad e_s^\top \bar{B}(\sigma) = e_s^\top A^{-1}B(\sigma) = e_s^\top. \quad (79)$$

b) *If also $\hat{A}e_1 = e_1$ and $c_1 = 0$ is satisfied, then*

$$A\mathbf{1} = e_1, \quad e_1^\top \tilde{B}(\sigma) = e_1^\top A^{-\top}B(\sigma)^\top = e_1^\top \quad (80)$$

Proof: a) Assumption $c_s = 1$ means that $e_s^\top V = \mathbf{1}^\top$. Hence,

$$\mathbf{1}^\top A = e_1^\top \hat{A}V^{-1} = \mathbf{1}^\top V^{-1} = e_s^\top.$$

Now, (28) also gives $\mathbf{1}^\top B(\sigma) = \mathbf{1}^\top A = e_s^\top$ and shows that the last row of the stability matrix satisfies $e_s^\top A^{-1}B(\sigma) = \mathbf{1}^\top B(\sigma) = e_s^\top$.

b) The assumption means $V^{-\top} \hat{A}e_1 = A\mathbf{1} = V^{-\top}e_1 = e_1$ since $e_1^\top V = e_1^\top$ for $c_1 = 0$. Hence, by (28) follows $B(\sigma)A^{-1}e_1 = B(\sigma)\mathbf{1} = A\mathbf{1} = e_1$. \square

Remark 5.1 Part a) of the Lemma shows that A has vanishing column sums with exception of the last one and that e_s^\top is the dominant left eigenvector of the stability matrix $\bar{B}(\sigma)$. Multiplying the time step (11) by A^{-1} we see that now the final stage of the standard Peer method reads

$$Y_{ns} = Y_{n-1,s} + h_n \sum_{j=1}^s \kappa_{jj} g(Y_{nj}, P_{nj}), \quad (81)$$

where $Y_{n-1,s} \cong y(t_n)$ since $c_s = 1$. Obviously, this last stage corresponds to the final one of a Runge-Kutta method and we call this form LSRK (Last Stage is Runge-Kutta). In fact, the quadrature weights of this stage do not depend on σ since $e_s^\top A^{-1} K = \mathbf{1}^\top K$, see (45). Under the assumptions of part b) of the Lemma stage number one of the adjoint time step, being the last step backwards, also is a final Runge-Kutta stage of the form

$$P_{n1} = P_{n+1,1} - h_n \sum_{j=1}^s \kappa_{jj} \varphi(Y_{nj}, P_{nj}), \quad (82)$$

since again $e_1^\top A^{-\top} K = \mathbf{1}^\top K$.

Compared to other candidates, the properties of such methods are surprisingly favorable since the LSRK form seems to decouple the two time steps to some extent which may weaken the difficulties brought by the σ -dependence of $\bar{B}(\sigma)$. Although (81), (82) look like simple Runge-Kutta end steps we stress the fact that the Peer method avoids order reduction by using the increments $g(Y_{nj}, U_{nj})$, $\varphi(Y_{nj}, U_{nj})$, $1 \leq j \leq s$, having high stage order due to their two-step structure.

It is a general observation in the design of numerical integrators that there may be a trade-off between accuracy requirements and stability properties. This happens also for Peer triplets and we will have to discuss different design choices. We remind of the general remark at the end of Section 3.2 that the knowledge of all necessary restriction for the boundary methods allows a detached development of the standard method having a small number of free parameters only. The choice of matching boundary methods may then follow up.

5.1 The triplet AP4o33vg for general grids

First, we discuss a method with orders $r = q = s - 1 = 3$ where both conditions (72) and (73) for super-convergence are cancelled σ -uniformly. Hence, there will be no smoothness restriction on the grids, only the usual bounds on the stepsize ratios, $\sigma_n \in [\underline{\sigma}, \bar{\sigma}]$, required by uniform zero stability. In our naming scheme from previous papers [11, 12], the triplet is denoted as AP4o33vg (**A**djoint **P**eer method with **4** stages and **orders 3,3** for **v**ariable stepsizes on **g**eneral grids). By Lemma 3.1 the necessary conditions for solvability of the combined conditions (52), (53) are fulfilled and a separate construction of the standard method is possible. Considering such Peer methods, the largest angles of $A(\alpha)$ -stability were observed with $c_1 = 0$ and $c_s = 1$. By Lemma 5.2 this means that the method has LSRK form forward and backward in time. In this situation, only 2 free parameters remain in (56), the node c_2 and $\hat{b}_{44}(\sigma)$ since the remaining entries of \hat{A} as well as c_3 are restricted by the required triangularity of A itself. The largest angle α was seen for $c_2 = \frac{1}{3}$ yielding a method of very simple form with

$$\mathbf{c}^\top = \left(0, \frac{1}{3}, \frac{2}{3}, 1\right), \quad K = \text{diag} \left(\frac{1}{8}, \frac{3}{8}, \frac{3}{8}, \frac{1}{8}\right), \quad A = \begin{pmatrix} 1 & 0 & 0 & 0 \\ -\frac{9}{4} & \frac{9}{4} & 0 & 0 \\ \frac{9}{4} & -\frac{9}{2} & \frac{9}{4} & 0 \\ -1 & \frac{9}{4} & -\frac{9}{4} & 1 \end{pmatrix}. \quad (83)$$

We note that the positive definite matrix K contains the weights of the *pulcherrima* quadrature rule associated with the given nodes in \mathbf{c} . With a fine-tuned choice of $\hat{b}_{44}(\sigma)$ the method possesses a stability angle of $\alpha \doteq 61.59$ and an interval of uniform zero stability $[\underline{\sigma}, \bar{\sigma}] = [0.57, 1.75]$ associated with the weight matrix W given in Appendix A1. The damping factor in (75) is $\gamma = 0.8$ and the error constants coincide $err_3 = err_3^\dagger \doteq 0.0093$. For later reference, we display the essential properties of the local errors in (30), (31) with $r = q = 3 = s - 1$ here:

$$\begin{aligned}\tau_n^Y &= h_n^r \beta_r(\sigma_n) y^{(r)}(t_n) + O(h_n^s \|y^{(s)}(t_n)\|_{[n]}), & \mathbb{1}^\top A \beta_r(\sigma) &\equiv 0 \text{ for all } \sigma, \\ \tau_n^P &= h_n^q \beta_q^\dagger(\sigma_{n+1}) p^{(q)}(t_n) + O(h_n^s \|p^{(s)}\|_{[n]}), & \mathbb{1}^\top A^\top \beta_q^\dagger(\sigma) &\equiv 0 \text{ for all } \sigma.\end{aligned}\tag{84}$$

A remarkable property of this method is that it coincides with its own adjoint, similar to the situation for BDF methods in [11, 18]. In fact, with the flip permutation $\Pi = (\delta_{i, s+1-i})$ it holds that $\Pi A \Pi = A^\top$ and $\Pi B(1) \Pi = B(1)^\top$ leading to the identity $\Pi A^{-1} B(1) \Pi = A^{-\top} B(1)^\top$ for the two stability matrices. As mentioned before, order 3 in the boundary steps is not possible with triangular matrices $K_n, A_n, n = 0, N$. In order to extend the symmetry of the standard method as far as possible, we kept the weight matrices $K_n \equiv K, n = 0, \dots, N$, and considered rank-1-perturbations for A_0 and A_N in block triangular form satisfying the order conditions for these methods. A very attractive choice is

$$A_0 = \begin{pmatrix} \frac{49}{80} & \frac{3}{4} & -\frac{3}{16} & 0 \\ -\frac{87}{80} & 0 & \frac{9}{16} & 0 \\ \frac{87}{80} & -\frac{9}{4} & \frac{27}{16} & 0 \\ -\frac{49}{80} & \frac{3}{2} & -\frac{33}{16} & 1 \end{pmatrix}, \quad A_N = \begin{pmatrix} 1 & 0 & 0 & 0 \\ -\frac{33}{16} & \frac{27}{16} & \frac{9}{16} & -\frac{3}{16} \\ \frac{3}{2} & -\frac{9}{4} & 0 & \frac{3}{4} \\ -\frac{49}{80} & \frac{87}{80} & -\frac{87}{80} & \frac{49}{80} \end{pmatrix} = (\Pi A_0 \Pi)^\top, \tag{85}$$

satisfying (78) with $\mu_0 = 2.7$. Since even the vectors from (12) and (13) are related by $w = \Pi a$ we see that the whole triplet coincides with its own adjoint. This is a very nice property and we will occasionally address this triplet **AP4p33vg** as *pulcherrima*. However, this beauty comes with a price, there are other triplets with much larger stability angles.

An overview of all standard methods and their essential properties is presented in Table 1 which displays the names of the triplets, the number of stages s , the orders (r, q) satisfied for all σ and the order r_1 satisfied for $\sigma = 1$ only, the range of the nodes, the stability angle α , the interval of stepsize ratios $[\underline{\sigma}, \bar{\sigma}]$ for which strong zero-stability (66) holds and finally the forward and adjoint error constants. Table 2 contains properties of the boundary methods, for instance the block form **blk_sz** of the matrices $K_n^{-1} A_n, n = 0, N$, which defines the size of the stage systems to be solved in these 2 time steps.

5.2 The triplet **AP4o33vs** for smooth grids

The LSRK property (79) for the state equation alone already leads to improved properties of the standard method. We now consider such methods with $r = q = s - 1 = 3$ where only the condition (72) is canceled σ -uniformly while the adjoint condition (73) is satisfied for $\sigma = 1$ only with the benefit of having 2 additional free parameters, \hat{a}_{s1} and c_1 .

Monte-Carlo-type computer searches, incorporating the construction of a suitable norm $\|\cdot\|$ in (65) in Section 4, found standard methods with stability angles of over 84 degrees. Restrictions on the damping factor (75) to $\gamma \leq 0.8$ and use of rational coefficients finally produced a standard method with angle $\alpha = 83.74$ for the triplet **AP4o33vs** for smooth grids. Here, the algebraic

restrictions from Lemma 3.2 lead to quite long algebraic expressions for all coefficients like

$$\mathbf{c}^\top = \left(\frac{144997}{389708}, \frac{73}{748}, \frac{77297572}{117896267}, 1 \right) \doteq (0.37207, 0.09759, 0.65564, 1), \quad (86)$$

with non-monotonic nodes. The quadrature weights in K are positive again in the interval $[0.11, 0.43]$. Since the coefficients of the triplet have very long rational representations, we will present them in double-precision only in Appendix A2. By a proper choice of $\hat{b}_{44}(\sigma)$ and a simplified weight matrix W , the interval of zero-stability in (65) becomes $[\underline{\sigma}, \bar{\sigma}] = [0.65, 1.80]$. The error constants, $err_3 \doteq 0.051$ and $err_3^\dagger \doteq 0.032$, are larger than for AP4o33vg, see Table 1. Here, the form of the local errors in (30), (31) with $r = q = 3$ is slightly different,

$$\begin{aligned} \tau_n^Y &= h_n^r \beta_r(\sigma_n) y^{(r)}(t_n) + O(h_n^s \|y^{(s)}(t_n)\|_{[n]}), & \mathbb{1}^\top A \beta_r(\sigma) &\equiv 0, \\ \tau_n^P &= h_n^q \beta_q^\dagger(\sigma_{n+1}) p^{(q)}(t_n) + O(h_n^s \|p^{(s)}\|_{[n]}), & \mathbb{1}^\top A^\top \beta_q^\dagger(\sigma) &= O(\sigma - 1). \end{aligned} \quad (87)$$

Since β_3^\dagger is a smooth function near $\sigma = 1$, we will show later that global order 3 still can be preserved for *smooth grids* satisfying $\sigma_n = 1 + O(h_n)$. Such grids are obtained naturally towards the end of adaptive grid generation strategies with successive refinements for sharper tolerances. Smooth grids are required for enhanced accuracy of the solutions only, but not by stability issues. In practice, the interval $[\underline{\sigma}, \bar{\sigma}] = [0.5, 1.8]$ of strong zero-stability should be comfortably large enough to enable the construction of coarse grids at the start of the computation.

For the boundary methods, it was again possible to choose $K_0 = K_N = K$ and the block triangular form seen in (85) where $\mu_0 = 5.1$, $\mu_N = 2.8$, see Table 2. The coefficients are also shown with real numbers in Appendix A.

5.3 A more accurate method satisfying additional order conditions

In our previous paper [12] it was observed that in many test problems the coupling between the errors in the state variable y and the multiplier p is rather weak for constant stepsizes. Methods satisfying more order conditions for the state y than for p indeed showed higher orders of convergence for y . Accordingly, we are now trying to increase the local order for the forward method beyond $r = s - 1$. By (57) additional conditions have to be solved with the elements of the last columns of \hat{A} and \hat{B} . Concentrating on the case $s = 4$ these matrices are given by (56) and (59). First of all, order 4 leads to $\hat{a}_{14} = 1$, i.e. $e_1^\top \hat{A} = \mathbb{1}^\top$. By (28), this leads to $e_1^\top \hat{B}(\sigma) = \mathbb{1}^\top = e_1^\top \mathcal{P}_s$ and shows that $e_1^\top \hat{B}(\sigma) \mathcal{P}_s^{-1} = e_1^\top \mathcal{Q}_{s,s} = e_1^\top$ and means that also $\mathcal{Q}_{2,s}$ possesses Hankel form. Hence, the conditions (52), (53) at the boundary are solvable even with $r = s$ for any such standard method. Now, the remaining residual of the full order condition (26) is

$$\hat{A} - \hat{K} \hat{E}_4 - \hat{B}(\sigma) P_4^{-1} S^{-1} = \begin{pmatrix} 0 \\ (\hat{a}_{24} - \frac{3}{4})(1 - \sigma^{-4}) \\ \hat{a}_{34}(1 - \sigma^{-5}) + (2\hat{a}_{24} - \frac{1}{2})\sigma^{-5} - \hat{k}_5(3 + 2\sigma^{-5}) \\ * \end{pmatrix} e_4^\top. \quad (88)$$

The last element in the column vector is not shown since it may be chosen arbitrarily with the remaining free parameter $\hat{b}_{44}(\sigma)$. Unfortunately, it seems that canceling the second entry in (88) uniformly in σ with the choice $\hat{a}_{24} = \frac{3}{4}$ leaves no $A(\alpha)$ -stable methods at all. Hence, we resorted to using the higher order $r_1 = 4$ in a restricted sense by canceling the residuals (88) for $\sigma = 1$ only with the choice

$$\hat{a}_{14} = 1, \quad \hat{a}_{24} = \frac{1}{4} + \frac{5}{2} \hat{k}_5. \quad (89)$$

This leaves only 5 parameters in \hat{A} . However, using also one degree of freedom from the nodes (see Lemma 3.2) algebra software was able to solve the equations for triangular form of the matrix $A = V^{-\top} \hat{A} V^{-1}$ formally. Extended computer searches in a three-parameter set of solutions found a very attractive standard method for the triplet **AP4o43vs** based on the node vector

$$\mathbf{c}^\top = \left(\frac{1}{2}(7 - \sqrt{29}), \frac{1}{2}, \frac{1}{10}(3 + \sqrt{29}), 1 \right) \doteq (0.0807, 0.5, 0.8385, 1). \quad (90)$$

We like to mention that the order 4 in the name refers to the global order of the scheme when applied to simple initial value problems without control. Since $c_s = 1$ and by (89) this is an LSRK-method by Lemma 5.2. It possesses a stability angle of $\alpha = 74.015^\circ$, small norm $\|\bar{B}(1)\|_\infty \doteq 1.63$, a good damping factor $|\lambda_2| \doteq 0.52$ and small error constants $err_4 \doteq 3.1 \cdot 10^{-3}$, $err_3^\dagger \doteq 0.076$. It also has positive quadrature weights

$$\mathbf{1}^\top K \doteq (0.23926055, 0.50765568, 0.16243097, 0.090652800) > 0^\top. \quad (91)$$

This method was designed with a moderate stepsize ratio $\hat{\sigma} = 1.2$ in the linear program (63) only, but it satisfies the norm estimate (65) in a larger interval. In order to avoid algebraic numbers in the norm $\|\cdot\|$, we constructed a simple rational approximation of its weight matrix as

$$W = \begin{pmatrix} 1 & -\frac{11}{6} & \frac{25}{6} & -\frac{7}{6} \\ 1 & -1 & -\frac{3}{2} & 1 \\ 1 & -\frac{1}{3} & -\frac{3}{2} & -\frac{2}{5} \\ 1 & 0 & 0 & 0 \end{pmatrix} \quad (92)$$

for which $W^{-1} \bar{B}(\sigma) W$ also has $1 + (s-1)$ block diagonal form (with a new lower block $B_{se}(\sigma)$) since it preserves the essential properties that $W e_1 = \mathbf{1}$ is the right eigenvector of \bar{B}^∞ and $e_1^\top W^{-1} = \mathbf{1}^\top A = e_s^\top$ its left eigenvector which means $e_s^\top W = e_1^\top$. The norms of the weight matrix and its inverse are $\|W\|_\infty \leq 8.2$ and $\|W^{-1}\|_\infty \leq 2$. With this weight matrix, the weight $W^\dagger = (AW)^{-\top}$ for P , and some fine-tuning of the parameter $\hat{b}_{44}(\sigma)$, the stability estimates (65) and (69)–(71) of the standard scheme with the nodes (90) hold in the interval $[\sigma, \bar{\sigma}] = [0.47, 1.79]$ with $\tilde{\gamma} \leq 0.984 < 1$. In fact, the function $\sigma \mapsto \|B_{se}(\sigma)\|_\infty$ consists of two monotone parts with minimum near $\sigma = 1.5$. Such norm estimates can even be proven rigorously by algebra software since only rational numbers and square roots are involved, by evaluating and bounding the relative maxima at the end points exactly. For instance, at $\sigma = 145/81 > 1.79$ and with a simple upper bound $\sqrt{29} \leq 727/135$, we have that $\|B_{se}(1.79)\|_\infty < 3767/3808 \doteq 0.989$.

The additional order conditions with $r_1 = 4$ for the boundary methods consume more free parameters from the matrices (A_0, K_0) and (A_N, K_N) and the following requirements could only be fulfilled with full 4×4 -block form. These criteria concern the error constants (76), (77), non-singularity of the step equation (78), and stability of the boundary steps. We denote this Peer triplet by **AP4o43vs** (4 stages, orders 4,3, variable stepsize, smooth grid). The essential data of the triplet are presented in Table 1 and its coefficients in Appendix A3. While the norm $\|A_N^{-1} B(1)\|$ for the end step of **AP4o43vs** equals one the norm $\|A_0^{-\top} B(1)^\top\| \cong 5.2$ for the starting step is still moderate. See Table 2 for further data of the boundary methods.

The LSRK property of the standard method in **AP4o43vs** leads to a further benefit for the local error since the condition for super-convergence of order s is satisfied for arbitrary σ . In (74) we get here

$$s! e_1^\top \hat{\beta}_s(\sigma) = s! \mathbf{1}^\top A \beta_s(\sigma) = (1 - \sigma^{-s})(\mathbf{1}^\top A c^s - 1) = (1 - \sigma^{-s})(c_s^s - 1) \equiv 0. \quad (93)$$

Hence, the adjoint local error corresponds to (87) but the error forward (30) with $r = q = 3 = s - 1$ is more involved, having the representation

$$\begin{aligned}\tau_n^Y &= h_n^r \beta_r(\sigma_n) y^{(r)}(t_n) + h_n^s \beta_s(\sigma_n) y^{(s)}(t_n) + O(h_n^{s+1} \|y^{(s+1)}\|_{[n]}), \\ \beta_r(\sigma) &= O(1 - \sigma), \quad \mathbf{1}^\top A \beta_r(\sigma) \equiv \mathbf{1}^\top A \beta_s(\sigma) \equiv 0.\end{aligned}\tag{94}$$

In principle, different negative powers of σ appear in $\|\beta_r(\sigma)\|$. However, all expressions vanish for $\sigma = 1$ and may be simply bounded by $|1 - \sigma|$ since $\sigma_n \in [\underline{\sigma}, \bar{\sigma}]$ by assumption.

5.4 An A-stable triplet AP4o33va

Although the stability angles of the previous Peer methods are sufficient for many problems, they do not qualify for A-stability. Since searches of A-stable standard methods of LSRK type with $q = r = s - 1 = 3$ were not successful, we resorted to considering Peer methods of general form. As in [12] it seems that A-stability requires entries of different signs in the coefficient matrix K and the diagonals of A and nodes outside of $[0, 1]$. Such methods still qualify for stiff problems as long as the diagonals of $K^{-1}A$ are positive with $\mu_n > 0$ in (78). When the orders $q = r$ coincide, one would usually look for methods with error constants $err_r \cong err_q^\dagger$ of equal magnitude. However, for A-stable methods the size of the adjoint error constant err_q^\dagger seems to be a bottleneck and we minimized the forward constant err_r with higher priority. The result was the following **A**-stable method **AP4o33va** for variable stepsizes based on the nodes

$$\mathbf{c}^\top = \left(0, \frac{53}{34}, \frac{6242}{30453}, \frac{298}{153}\right) \doteq (0, 1.5588, 0.2050, 1.9477)$$

with a forward error $err_3 \doteq 0.013$ and a larger adjoint error $err_3^\dagger \doteq 0.88$. Since the left eigenvector of \bar{B}^∞ is not as simple for **AP4o33va** as $\mathbf{1}^\top A = e_s^\top$ for LSRK methods and now has long rational expressions, there is no simple rational approximation for the weight matrix W . With the weight given in Appendix A4 the method is uniformly zero-stable in the norm (65) for $\sigma \in [0.61, 1.52]$, with a good damping factor $|\lambda_2| \doteq 0.29$, see also Table 1. Although $\|\bar{B}(1)\| = 1$ holds by design, the row sum norm $\|\bar{B}(1)\|_\infty \doteq 20.1$ is rather large and may lead to some susceptibility for rounding errors if sharp tolerances are applied. The size of this norm may be due to the necessity for large entries in the last row of $\hat{B}(\sigma)$ which seem to be required by A-stability, see Appendix A4. The local errors (30), (31) with $r = q = 3 = s - 1$ for the standard method satisfy,

$$\begin{aligned}\tau_n^Y &= h_n^r \beta_r(\sigma_n) y^{(r)}(t_n) + O(h_n^s \|y^{(s)}(t_n)\|_{[n]}), & \mathbf{1}^\top A \beta_r(\sigma) &= O(1 - \sigma), \\ \tau_n^P &= h_n^q \beta_q^\dagger(\sigma_{n+1}) p^{(q)}(t_n) + O(h_n^s \|p^{(s)}\|_{[n]}), & \mathbf{1}^\top A^\top \beta_q^\dagger(\sigma) &= O(1 - \sigma).\end{aligned}\tag{95}$$

The additional restrictions again seem to prohibit the existence of boundary methods with some reduced block structure and $K_0^{-1}A_0, K_N^{-1}A_N$ are full matrices. As for the standard method the adjoint error constants are quite large for these steps, too, see Table 2. Although the row resp. column sum norms of the exceptional stability matrices are also quite large, their stability norms still are quite moderate $\|A_0^{-\top} B(1)^\top\| \doteq 2.7, \|A_N^{-1} B(1)\| \doteq 2.2$.

6 Convergence

Since convergence for variable stepsizes requires more advanced arguments than in our previous papers [11, 12], we prove it here again. An important difficulty comes from the two-step form of the

triplet	$s, (r, q)$	r_1	nodes	α	$\sigma \in$	$ \lambda_2 $	err_{r_1}	err_q^\dagger
AP4o33vg	4, (3, 3)	3	[0, 1]	61.59 $^\circ$	[0.57, 1.80]	0.31	9.8e-3	9.8e-3
AP4o33vs	4, (3, 3)	3	(0, 1]	83.74 $^\circ$	[0.65, 1.80]	0.80	5.1e-2	3.2e-2
AP4o43vs	4, (3, 3)	4	(0, 1]	74.01 $^\circ$	[0.47, 1.79]	0.52	3.1e-3	7.6e-2
AP4o33va	4, (3, 3)	3	[0, 1.95]	90 $^\circ$	[0.61, 1.52]	0.29	1.3e-2	8.8e-1

Table 1: Essential properties of the standard methods of Peer triplets.

triplet	Starting method					End method				
	blksz	q_b	μ_0	$err_{r_1,0}$	$err_{q,0}^\dagger$	blksz	q_b	μ_N	$err_{r_1,N}$	$err_{q,N}^\dagger$
AP4o33vg	3+1	∞	2.74	1.1e-2	8.2e-3	1+3	∞	2.74	4.4e-2	8.2e-3
AP4o33vs	3+1	∞	5.18	9.4e-3	2.1e-2	1+3	∞	2.84	5.4e-2	2.7e-2
AP4o43vs	4	2	3.73	1.2e-3	8.4e-2	4	2	2.93	3.4e-3	7.2e-3
AP4o33va	4	2	1.81	3.1e-2	0.77	4	2	0.67	5.6e-2	1.17

Table 2: Properties of the boundary methods of Peer triplets.

Peer methods leading to σ -dependent stability matrices in the numerical solution of the boundary problem (8), (9).

Inheriting the index range from the grid, we denote the numerical solution by $Y = (Y_n)_{n=0}^N$, $P = (P_n)_{n=0}^N$, and the vector of exact solutions in boldface $\mathbf{y} = (\mathbf{y}_n)_{n=0}^N$, $\mathbf{p} = (\mathbf{p}_n)_{n=0}^N$, where $\mathbf{y}_n = (y^*(t_{nj})_{j=1}^s)$, $\mathbf{p}_n = (p^*(t_{nj})_{j=1}^s)$, $0 \leq n \leq N$. The global errors are indicated with checks, $\check{Y} = Y - \mathbf{y}$, $\check{P} = P - \mathbf{p}$. For ease of writing, we also introduce the combined error vector $\check{Z} = (\check{Y}^\top, \check{P}^\top)^\top$. For the following analysis of the discrete boundary value problem, we multiply the equations (19), (20) by appropriate inverses A_n^{-1} , and multiply (22), (23) likewise by $A_n^{-\top}$. Comparing them with the residuals in these equations when the exact solution \mathbf{z} is the argument, we obtain the following error equations:

$$\check{Y}_n - \bar{B}_n \check{Y}_{n-1} = R_n^Y(\check{Z}) - \tau_n^Y, \quad n = 0, \dots, N, \quad (96)$$

$$R_n^Y(\check{Z}) := h_n \bar{K}_n (G(\mathbf{z}_n + \check{Z}_n) - G(\mathbf{z}_n)),$$

$$\check{P}_n - \tilde{B}_{n+1}^\top \check{P}_{n+1} = R_n^P(\check{Z}) - \tau_n^P, \quad n = 0, \dots, N-1, \quad (97)$$

$$R_n^P(\check{Z}) := -h_n A_n^{-\top} (\Phi(\mathbf{y}_n + \check{Y}_n, K_n^\top(\mathbf{p}_n + \check{P}_n)) - \Phi(\mathbf{y}_n, K_n^\top \mathbf{p}_n)),$$

Here, τ_n^Y, τ_n^P are the truncation errors computed in (30), (31) and $\bar{K}_n = A_n^{-1} K_n$. The error equation for the starting step is covered by (96) by setting $\bar{B}_0 = 0$. For simplicity, the adjoint

Time steps	state	adjoint	
	order $r < s$	order $q < s$,	q_b
(a) Start, $n=0$	(46)	(25), (54),	(33)
(b) Standard, $1 \leq n < N$	(26)	(25)	
(c) Super-convergence	(72)=0	(73)=0	
(d) matching condition	(36)		
(e) last step, $n = N$	(26), (51)	(49),	(33)

Table 3: Combined order conditions for the peer triplets.

boundary condition (23) is only considered for polynomial objective functions of degree 2 at most. Here, the error equation reads

$$\begin{aligned} \check{P}_N - ((\mathbb{1}w^\top) \otimes \nabla_{yy}C) \check{Y}_N &= R_N^P(\check{Z}) - \tau_N^P, \\ R_N^P(\check{Z}) &:= -h_N A_N^{-\top} (\Phi(\mathbf{y}_N + \check{Y}_N, K_N^\top(\mathbf{p}_N + \check{P}_N)) - \Phi(\mathbf{y}_N, K_N^\top \mathbf{p}_N)). \end{aligned} \quad (98)$$

Combining all equations leads to a nonlinear system for the global error of the form

$$\mathbb{M}_0 \check{Z} = -\tau + R(\check{Z}) := \begin{pmatrix} -\tau^Y + R^Y(\check{Z}) \\ -\tau^P + R^P(\check{Z}) \end{pmatrix}. \quad (99)$$

The matrix \mathbb{M}_0 contains all parts on the left-hand sides of (96)–(98) being independent of the stepsizes h_n . It has block triangular form (see also [11, 12])

$$\mathbb{M}_0 = \begin{pmatrix} M_{11} \otimes I_m & 0 \\ M_{21} \otimes \nabla_{yy}C & M_{22} \otimes I_m \end{pmatrix}, \quad \mathbb{M}_0^{-1} = \begin{pmatrix} M_{11}^{-1} \otimes I_m & 0 \\ -M_{22}^{-1} M_{21} M_{11}^{-1} \otimes \nabla_{yy}C & M_{22}^{-1} \otimes I_m \end{pmatrix}. \quad (100)$$

Due to the two-step form of the Peer methods, the matrix M_{11} is lower block triangular and M_{22} is upper block triangular with identities I_s in the main diagonal and the stability matrices $\bar{B}_n := A_n^{-1} B_n$, $1 \leq n \leq N$, respectively $\tilde{B}_{n+1}^\top := A_n^{-\top} B_{n+1}^\top$, $0 \leq n < N$, in the first off-diagonals. Of great interest for the analysis is the precise form of their inverses which is explicitly given by ([11])

$$(M_{11}^{-1})_{nk} = \bar{B}_n \cdots \bar{B}_{k+1}, \quad k < n, \quad (M_{22}^{-1})_{nk} = \tilde{B}_{n+1}^\top \cdots \tilde{B}_k^\top, \quad k > n, \quad (101)$$

with identities in the main diagonal again. The matrix M_{21} has nontrivial entries of rank-one form in the very last block only, $(M_{21})_{NN} = -\mathbb{1}w^\top$. Since $\mathbb{1}$ is an eigenvector for all matrices \bar{B}_n and $w^\top A_N^{-1} = \mathbb{1}^\top$ by (49), the southwest block in \mathbb{M}_0^{-1} is quite simple since $M_{22}^{-1} M_{21} M_{11}^{-1} = (\mathbb{1}_N \otimes \mathbb{1}_s)(\mathbb{1}_N \otimes \mathbb{1}_s)^\top$ is a matrix of ones.

For the error analysis it is of utmost importance that the products in (101) are uniformly bounded. Hence we need to use vector norms associated with the weighted matrix norms (65), (66) from Section 4 whose construction is part of the triplet design process itself. The vector norms are defined by

$$\|Y\| := \max_n \|W^{-1} Y_n\|_\infty, \quad \|P\| := \max_n \|(W^\dagger)^{-1} P_n\|_1, \quad \|Z\| := \max \{\|Y\|, \|P\|\}, \quad (102)$$

where $\|W^{-1} Y_n\|_\infty = \|(W \otimes I_m)^{-1} Y_n\|_\infty$ means the maximum norm and $\|\cdot\|_1$ the sum norm in the stage space, the norm in the state space \mathbb{R}^m may be chosen by convenience.

Applying the Banach Fixed Point Theorem to the error equations (96), etc, requires bounds on the derivatives of the right-hand sides g, ϕ of the reduced problem (8), (9). Hence, we assume that constants Λ exist such that

$$\|\nabla_y g\| \leq \Lambda_y, \quad \|\nabla_p g\| \leq \Lambda_p, \quad \|\nabla_y \phi\| \leq \Lambda_y^\dagger, \quad \|\nabla_p \phi\| \leq \Lambda_p^\dagger, \quad (103)$$

in some open tubular neighbourhood of the exact solution (y, p) of (8), (9). We also introduce $\Gamma := \|\nabla_{yy}C\|$ which vanishes for linear objective functions.

An important aspect of our error estimates is localized bounds containing terms like $h_n^r \|y^{(r)}\|_{[n]}$ which may show the potential for equidistribution of errors in practical computations. Although the usual order conditions (26), (27) are valid for any $r, q \leq s \in \mathbb{N}$ the one-leg-condition (33) have been derived for $q_b \leq 2$ only in [12]. The corresponding assumption may be a limitation for triplets where K_0, K_N do not have diagonal form, see Table 2.

Theorem 6.1 Assume that the Peer triplet satisfies the order conditions from the lines (a), (b), (d), (e) of Table 3 with $2 \leq r = q < s$ and $q - 1 \leq q_b \leq 2$, for arbitrary $\sigma \in \mathbb{R}$ and that there exists a norm such that $\|\bar{B}(\sigma)\| = \|\tilde{B}(\sigma)^\top\| = 1$ for $\sigma \in [\underline{\sigma}, \bar{\sigma}]$, $1 \leq n < N$, see (65), (66). Let the solution of the problem (8), (9) satisfy $y, p \in C^r[0, T^*]$ and the upper bounds (103) the conditions

$$(\zeta_y \Lambda_y + \zeta_p \Lambda_p)T \leq \frac{1}{2}, \quad (\zeta_y^\dagger \Lambda_y^\dagger + \zeta_p^\dagger \Lambda_p^\dagger + \frac{s}{2}\Gamma)T \leq \frac{1}{2}, \quad (104)$$

with constants ζ, ζ^\dagger which depend only on the coefficients of the Peer triplet. Let the objective function \mathcal{C} be polynomial with degree not exceeding two.

Then, applying the Peer triplet on a grid with stepsize ratios $\sigma_n \in [\underline{\sigma}, \bar{\sigma}]$, $0 < \underline{\sigma} < 1 < \bar{\sigma}$, and a sufficiently small $H = \max_n h_n$, its errors satisfy

$$\|\tilde{Z}\| = \max\{\|Y - \mathbf{y}\|, \|P - \mathbf{p}\|\} \leq \mu \left(\max_n h_n^{r-1} \|y^{(r)}\|_{[n]} + \max_n h_n^{q-1} \|p^{(q)}\|_{[n]} \right). \quad (105)$$

Proof: The error equation (99) may be written in fixed point form

$$\tilde{Z} = \Psi(\tilde{Z}) := -\mathbb{M}_0^{-1}\tau + \mathbb{M}_0^{-1}R(\tilde{Z}). \quad (106)$$

Considering Lipschitz differences of the right-hand sides R_n^Y, R_n^P with sufficiently small \tilde{Z}, \hat{Z} , we get

$$R_n^Y(\tilde{Z}) - R_n^Y(\hat{Z}) = h_n \bar{K}_n (\nabla_Y G_n \cdot (\tilde{Y}_n - \hat{Y}_n) + \nabla_P G_n \cdot (\tilde{P}_n - \hat{P}_n)), \quad (107)$$

where, e.g., $\nabla_Y G_n$ is a block-diagonal matrix of integral means, $\int_0^1 \nabla_y g((1-t)\tilde{Y}_{nj} + t\hat{Y}_{nj})dt$, $j = 1, \dots, s$. And for R_n^P we get likewise

$$R_n^P(\tilde{Z}) - R_n^P(\hat{Z}) = -h_n A_n^{-\top} (\nabla_Y \Phi_n \cdot (\tilde{Y}_n - \hat{Y}_n) + \nabla_P \Phi_n \cdot K_n^\top (\tilde{P}_n - \hat{P}_n)). \quad (108)$$

For the Lipschitz constant of Ψ , we have to consider the multiplication with \mathbb{M}_0^{-1} , and for realistic bounds, the use of the weighted norms (102) is required, which are different for Y and P . Since the handling of $M_{11}^{-1} \bar{K}_n \nabla_Y G_n$ is straight-forward, we consider the second term in (107) in more detail. By assumption, in (101) we have $\|\bar{B}_n\| = \|W \bar{B}_n W^{-1}\|_\infty = 1$ with the possible exception for $n = 0$ or $n = N$. Since B_N is a common factor in the last block row of of the lower block tringular matrix M_{11}^{-1} , whose norm may exceed one, we show the left-most factor in the following estimate separately,

$$\begin{aligned} \|\|M_{11}^{-1} (h_n \bar{K}_n \nabla_P G_n \cdot (\tilde{P}_n - \hat{P}_n))_{n=0}^N\| &\leq \max_n \|B_n\| \sum_{k=0}^n h_k \|W^{-1} \bar{K}_k \nabla_P G_k (\tilde{P}_k - \hat{P}_k)\|_\infty \\ &\leq \|B_N\| \|W^{-1} \bar{K}\|_\infty (O(h_0) \|\tilde{P}_0 - \hat{P}_0\|_\infty + \sum_{k=1}^N h_k \|(\tilde{P}_k - \hat{P}_k)\|_\infty) \\ &\leq \|B_N\| \|W^{-1} \bar{K}\|_\infty (O(H) + T \max_{i,j} |w_{ij}^\dagger|) \|\tilde{P} - \hat{P}\|. \end{aligned}$$

In the last step the factor $\max_{i,j} |w_{ij}^\dagger|$ appears due to the switch to the 1-norm for P . Defining constants $\zeta_p := 2 \|B_N\| \|W^{-1} \bar{K}\|_\infty \max_{i,j} |w_{ij}^\dagger|$, and ζ_y in a similar way, we get the Lipschitz estimate

$$\|\|M_{11}^{-1} (R^Y(\tilde{Z}) - R^Y(\hat{Z}))\| \leq (\zeta_y \Lambda_y + \zeta_p \Lambda_p)T \|\tilde{Z} - \hat{Z}\| \quad (109)$$

for H small enough. We note that, like the given example ζ_p , all ζ -constants only depend on the coefficients of the Peer triplet.

For the product of M_{22}^{-1} and (108), we obtain in a similar way

$$\|M_{22}^{-1}(R^P(\tilde{Z}) - R^P(\hat{Z}))\| \leq (\zeta_y^\dagger \Lambda_y^\dagger + \zeta_p^\dagger \Lambda_p^\dagger) T \|\tilde{Z} - \hat{Z}\|, \quad (110)$$

where the norm on the left-hand side is $\|(W^\dagger)^{-1} \cdot\|_1 = \|W^\top A^\top \cdot\|_1$ and now $\|\tilde{B}_1^\top\| \geq 1$ may be an exceptional factor in $\zeta_y^\dagger, \zeta_p^\dagger$. Since $(W^\dagger)^{-1} \mathbf{1} = e_1$, the southwest block in M_0^{-1} also contributes

$$\sum_{n=0}^N \|(\mathbb{1}_s^\top \otimes \nabla_{yy} \mathcal{C})(R_n^Y(\tilde{Z}) - R_n^Y(\hat{Z}))\| \leq s \|\nabla_{yy} \mathcal{C}(\zeta_y \Lambda_y + \zeta_p \Lambda_p) T\| \|\tilde{Z} - \hat{Z}\|. \quad (111)$$

This leads to the additional term in the second part of assumption (104). Summing up, by assumption (104), we have shown that Ψ is a contraction

$$\|\Psi(\tilde{Z}) - \Psi(\hat{Z})\| \leq \frac{1}{2} \|\tilde{Z} - \hat{Z}\|. \quad (112)$$

The truncation errors τ^Y, τ^P presented in (30), (31) are multiplied in $\Psi(0) = -M_0^{-1} \tau$ by the block matrix from (100). Bounding this multiplication straightforward, one power of h_n^r is lost and we get $\|\Psi(0)\| \leq (\mu/2) (\max_n h_n^{r-1} \|y^{(r)}\|_{[n]} + \max_n h_n^{q-1} \|p^{(q)}\|_{[n]})$ with some constant μ . By standard arguments we see that a closed neighborhood $\{\tilde{Z} : \|\tilde{Z}\| \leq \varepsilon\}$ of the origin is mapped onto itself for $\|M_0^{-1} \tau\| = O(H^{r-1}) \leq \varepsilon/4$ and finally, that the fixed point \tilde{Z} in (106) is bounded by

$$\|\tilde{Z}\| \leq 2 \|\Psi(0)\| = 2 \|M_0^{-1} \tau\|, \quad (113)$$

since $\|\tilde{Z}\| - \|\Psi(0)\| \leq \|\tilde{Z} - \Psi(0)\| = \|\Psi(\tilde{Z}) - \Psi(0)\| \leq \frac{1}{2} \|\tilde{Z}\|$. \square

With the first estimate from Theorem 6.1, we may now prove higher order error estimates. According to (113) this is accomplished by refining the bound for $\|M_0^{-1} \tau\|$ employing super-convergence effects according to the conditions from line (d) in Table 3. The situation is more difficult than in previous papers since these conditions may be fulfilled for constant stepsizes only, i.e. $\sigma = 1$. We remind that different Peer triplets correspond to different choices of the parameters $\hat{a}_{1s}, \hat{a}_{s1}$ in Lemma 6.1. However, super-convergence is quite robust and is well observed in our numerical tests since good grid strategies lead to stepsize ratios σ_n clustering near one for shrinking tolerances. The following lemma takes account of this by considering *smooth grids* with $\sigma_n = 1 + O(h_n)$ for all stepsize ratios in the grid.

Due to super-convergence, the error estimates will depend on several derivatives of the solutions. In order to shorten these expressions, we introduce the following Matlab-type abbreviation for Sobolev semi-norms of a sufficiently smooth function $v(t)$,

$$\|v^{(r_1:r_2)}\|_{[n]} := \max_{k=r_1, \dots, r_2} \|v^{(k)}\|_{[n]}, \quad r_1 \leq r_2. \quad (114)$$

Lemma 6.1 *Let the assumptions of Theorem 6.1 be satisfied with $q = r = s - 1$ and let $y, p \in C^s[0, T^*]$.*

a) *For methods canceling both super-convergence conditions (72), (73) uniformly in σ the errors are bounded by*

$$\max\{\|Y - \mathbf{y}\|, \|P - \mathbf{p}\|\} \leq \mu \left(\max_n h_n^{s-1} \|y^{(s-1:s)}\|_{[n]} + \max_n h_n^{s-1} \|p^{(s-1:s)}\|_{[n]} \right), \quad (115)$$

with some constant $\mu > 0$.

b) If all stepsize ratios of the grid also satisfy $\sigma_n = 1 + O(h_n)$, $1 \leq n \leq N$, the error estimate (115) still holds if the method cancels (72), (73) for $\sigma = 1$ only.

Proof: The improved error estimates will follow by refining the estimates for $\mathbb{M}_0^{-1}\tau$ in (113). Since the main difference between our first two methods concerns the adjoint error, we consider $\epsilon^P := M_{22}^{-1}\tau^P$ in more detail. By (31), we have $\tau_n^P = h_n^q \beta_q^\dagger(\sigma_{n+1})p^{(q)}(t_n) + O(h_n^s \|p^{(s)}\|_{[n]})$. Also, by (73) holds $q!(\tilde{B}^\infty)^\top \beta_q^\dagger(\sigma) = \hat{a}_{s1}(1 - \sigma^q)\mathbb{1}$ where $(\tilde{B}^\infty)^\top = \mathbb{1}\mathbb{1}^\top A^\top$. Separating the term with the exceptional matrix \tilde{B}_N^\top , where $\|\tilde{B}_N^\top\|$ may exceed one, we obtain with some positive constant μ_1 that

$$\begin{aligned}
\|\epsilon_n^P\| &= \|\tau_n^P + \sum_{k=n+1}^{N-1} \tilde{B}_{n+1}^\top \cdots \tilde{B}_k^\top \tau_k^P + \tilde{B}_{n+1}^\top \cdots \tilde{B}_N^\top \tau_N^P\| \\
&\stackrel{(66)}{\leq} \|\tau_n^P\| + \sum_{k=n+1}^{N-1} \|(\tilde{B}^\infty)^\top \tau_k^P\| + \sum_{k=n+1}^{N-1} \|(\tilde{B}_{n+1}^\top \cdots \tilde{B}_k^\top \tau_k^P - (\tilde{B}^\infty)^\top \tau_k^P)\| + \|\tilde{B}_N^\top \tau_N^P\| \\
&\stackrel{(71)}{\leq} \mu_1 \left(h_n^q \|p^{(q)}\|_{[n]} + h_N^q \|p^{(q)}\|_{[N]} \right. \\
&\quad \left. + \sum_{k=n+1}^{N-1} (|\hat{a}_{s1}| |1 - \sigma_{k+1}| h_k^q \|p^{(q)}(t_k)\| + h_k^s \|p^{(s)}\|_{[k]} + \tilde{\gamma}^{k-n} h_k^q \|p^{(q)}\|_{[k]}) \right) \\
&\leq \mu_1 \left(2 + \sum_{k=n+1}^{N-1} (|\hat{a}_{s1}| |1 - \sigma_{k+1}| + h_k + \tilde{\gamma}^{k-n}) \right) \max_n h_n^q \|p^{(q;s)}\|_{[n]}. \tag{116}
\end{aligned}$$

It is obvious that the constant in brackets is uniformly bounded for $\hat{a}_{s1} = 0$ without restrictions on σ_{k+1} since $\tilde{\gamma} < 1$. The corresponding estimate for $\epsilon^Y := M_{11}^{-1}\tau^Y$ follows in the same way by separating the contribution from the exceptional matrix \tilde{B}_1 and using (30), (69) where (72) leads to a term $|\hat{a}_{1s} - 1| \sum_{k=1}^n |1 - \sigma_k|$, which vanishes for $\hat{a}_{1s} = 1$.

The contribution to \mathbb{M}_0^{-1} from the subdiagonal matrix block $M_{21} = (e_N \otimes \mathbb{1})(e_N \otimes w)^\top$, which has entries in the very last diagonal block only, is

$$-((M_{22}^{-1}M_{21}M_{11}^{-1}) \otimes \nabla_{yy}\mathcal{C})\tau^Y = -\mathbb{1}_{s(N+1)} \otimes (\nabla_{yy}\mathcal{C}(w^\top \otimes I_m)\epsilon_N^Y).$$

It is obviously bounded by $O(\|\epsilon^Y\|)$. Summarizing, we have that without further restrictions on all σ_n it holds that $\epsilon^Y = O(h^q)$ only for methods with $\hat{a}_{1s} = 1$ and $\epsilon^P = O(h^q)$ only for methods with $\hat{a}_{s1} = 0$. Since the smallest order dominates the final estimate (113), only methods possessing both properties are covered by case a) of the assertion. The other methods require the strengthened assumption from part b), which yields $|1 - \sigma_k| = O(h_k)$. \square

Remark 6.1 a) We note that $\hat{a}_{1s} = 1$ for all LSRK methods.

b) The estimate (116) and the discussion for ϵ^Y show that the restriction on the stepsize ratios in part b) of the lemma may be weakened to

$$\sum_{n=1}^N |1 - \sigma_n| \leq \text{const}$$

which would allow a uniformly bounded number of exceptions from the rule $\sigma_n = 1 + O(h_n)$.

c) The assumption $\sigma_n = 1 + O(h_n)$ may seem quite restrictive in practice. However, considering sequences of the form $h_{n+1} = h_n(1 + \mu h_n)$, $h_0, \mu > 0$, it is easy to prove inductively that

$$h_n \geq h_0 \prod_{j=1}^n (1 + \mu h_0(1 + \mu h_0)^{j-1}) \geq h_0(1 + \mu h_0)^n$$

showing that more than an exponential increase of stepsizes is still possible.

Using the detailed information on the triplets from (84), (87), (94), (95) and Table 1 and 2, we obtain

Corollary 6.1 *The error estimate (115) of Lemma 6.1 holds with $r = q = 3$ for the triplets*

a) *APv4o33vg for stepsize ratios $\sigma_n \in [\underline{\sigma}, \bar{\sigma}] = [0.5, 1.8]$,*

b) *APv4o33vs, APv4o43vs, APv4o33va for stepsize ratios $\sigma_n = 1 + O(h_n) \in [\underline{\sigma}, \bar{\sigma}]$ with the intervals $[\underline{\sigma}, \bar{\sigma}]$ displayed in Table 1.*

Remark 6.2 *The last corollary 6.1 does not contain a statement on improved convergence properties of the triplet AP4o43vs. This is because the error structure (94) only suffices to show $\epsilon^Y = O(h^4)$ while ϵ^P remains with order 3. As stated at the end of the proof of the last lemma, the smallest order dominates the general estimate (113). However, in our previous papers and our numerical tests, we observed that in many problems the coupling between the errors of the state variable y and that of p seems to be rather weak and test results show the higher order for the state indeed.*

In order to justify our claim we shortly sketch an estimate for ϵ^Y . With (94), (101), $\bar{B}^\infty = \mathbf{1}\mathbf{1}^\top A$ and neglecting for simplicity the case of an exceptional \bar{B}_1 , we get with positive constants μ , μ_1 , and μ_2 ,

$$\begin{aligned} \|\epsilon_n^Y\| &= \left\| \sum_{k=0}^{n-1} \bar{B}_n \cdots \bar{B}_{k+1} \tau_k^Y + \tau_n^Y \right\| \\ &\leq \sum_{k=0}^{n-1} \|\bar{B}^\infty \tau_k^Y\| + \sum_{k=0}^{n-1} \|(\bar{B}_n \cdots \bar{B}_{k+1} - \bar{B}^\infty) \tau_k^Y\| + \|\tau_n^Y\| \\ &\stackrel{(94)}{\leq} \mu_1 \left(\sum_{k=0}^{n-1} (h_k^5 \|y^{(5)}\|_{[k]} + \tilde{\gamma}^{n-k} (h_k^3 |1 - \sigma_k| \|y^{(3)}\|_{[k]} + h_k^4 \|y^{(4)}\|_{[k]})) \right. \\ &\quad \left. + h_n^3 |1 - \sigma_n| \|y^{(3)}\|_{[n]} + h_n^4 \|y^{(4)}\|_{[n]} \right) \\ &\leq \mu_2 \left(2 + \sum_{k=0}^{n-1} (h_k + \tilde{\gamma}^{n-k}) \right) \max_n h_n^4 \|y^{(3;5)}\|_{[n]} \leq \mu \max_n h_n^4 \|y^{(3;5)}\|_{[n]}, \end{aligned}$$

for smooth grids satisfying $|1 - \sigma_k| = O(h_k)$ for all k . This estimate shows that the standard method AP4o43vs possesses order 4 for pure initial value problems for the state variable without control.

7 Numerical tests

We present numerical results for all Peer triplets listed in Table 1. All calculations have been done with Matlab-Version R2021a, using the nonlinear solver *fsolve* to approximate the overall coupled scheme (19)–(23) with a tolerance 10^{-14} . To illustrate the rates of convergence and efficiency of variable stepsizes, we consider two nonlinear unconstrained optimal control problems with inherent boundary layers and known exact solutions.

7.1 Nonlinear problem

The first problem reads:

$$\begin{aligned}
& \text{Minimize } y_3(0.5) \\
& \text{subject to } \begin{aligned}
& y_1'(t) = y_1^2(t) - 2y_1(t)y_2(t) + y_2^2(t) + \lambda u(t), \\
& y_2'(t) = \lambda y_2(t), \\
& y_3'(t) = 0.5(y_1(t) - y_d(t))^2 + 0.5\alpha(u(t) - u_d(t))^2, \quad t \in (0, 0.5], \\
& y_1(0) = 2, \quad y_2(0) = 1, \quad y_3(0) = 0,
\end{aligned}
\end{aligned}$$

with $y_d(t) = \exp(\lambda t) + (1 - t)^{-1}$ and $u_d(t) = \exp(\lambda t)$. Integrating the equation with $y_3'(t)$ over $[0, 0.5]$ and replacing $y_3(0.5)$ in the objective function shows that the optimal control is of so-called tracking type minimizing the integral $\frac{1}{2} \int_0^{0.5} ((y_1 - y_d)^2 + \alpha(u - u_d)^2) dt$. The adjoint equations are

$$\begin{aligned}
p_1'(t) &= -2(y_1(t) - y_2(t))p_1(t) - (y_1(t) - y_d(t))p_3(t), \\
p_2'(t) &= -2(y_2(t) - y_1(t))p_1(t) - \lambda p_2(t), \\
p_3'(t) &= 0, \quad t \in (0, 0.5], \\
p_1(0.5) &= 0, \quad p_2(0.5) = 0, \quad p_3(0.5) = 1.
\end{aligned}$$

Observe the trivial solution $p_3(t) = 1$. Hence, the optimality condition

$$\nabla_u f(y, u)^T p = \lambda p_1 + \alpha(u - u_d)p_3 = 0$$

can be used to calculate the optimal control from $u = u_d - \lambda p_1 / (\alpha p_3)$, which gives the boundary value problem (with eliminated control)

$$\begin{aligned}
y_1'(t) &= y_1^2(t) - 2y_1(t)y_2(t) + y_2^2(t) + \lambda \left(u_d(t) - \frac{\lambda p_1(t)}{\alpha p_3(t)} \right), \\
y_2'(t) &= \lambda y_2(t), \\
y_3'(t) &= 0.5(y_1(t) - y_d(t))^2 + 0.5\alpha \left(\frac{\lambda p_1(t)}{\alpha p_3(t)} \right)^2, \\
p_1'(t) &= -2(y_1(t) - y_2(t))p_1(t) - y_1(t) + y_d(t), \\
p_2'(t) &= -2(y_2(t) - y_1(t))p_1(t) - \lambda p_2(t), \\
p_3'(t) &= 0, \quad t \in (0, 0.5], \\
y_1(0) &= 2, \quad y_2(0) = 1, \quad y_3(0) = 0, \quad p_1(0.5) = 0, \quad p_2(0.5) = 0, \quad p_3(0.5) = 1.
\end{aligned}$$

The exact solutions are $y_1(t) = \exp(\lambda t) + (1 - t)^{-1}$, $y_2(t) = \exp(\lambda t)$, $y_3(t) = 0$, $p_1(t) = p_2(t) \equiv 0$, $p_3(t) = 1$. The components $y_1(t)$ and $y_2(t)$ exhibit the same exponential boundary layer structure at $t = 0$. We choose $\lambda = -50$ (mildly stiff regime) and set $\alpha = 1$.

7.1.1 Stepsize sequences with alternating and smoothly varying σ

In order to study the rates of convergence under stiffness and changing step sizes, we first consider alternating stepsize sequences depending on a fixed parameter σ according to

$$h_0 = \frac{2h}{\sigma + 1}, \quad h_n = h_{n-1} \sigma^{(-1)^{n-1}}, \quad n = 1, 2, \dots, N - 1,$$

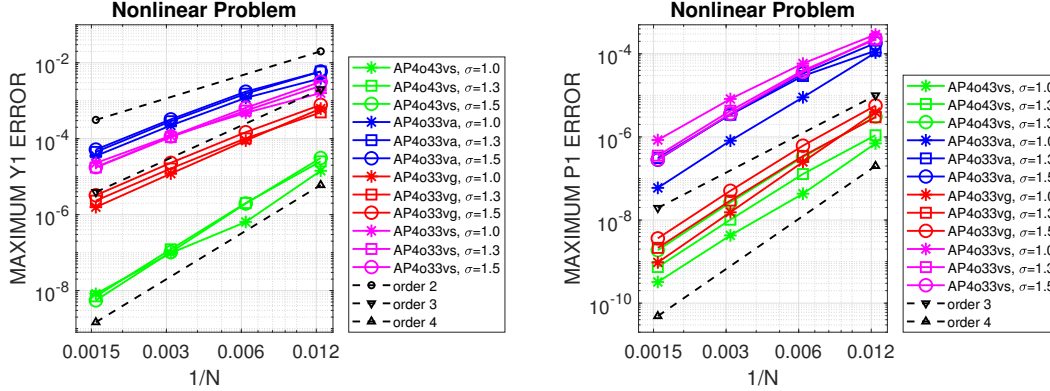


Figure 1: Test with alternating meshes and fixed $\sigma = 1.0, 1.3, 1.5$. Convergence of the maximal state errors $\|Y_{1,ni} - y_1(t_{ni})\|_\infty$ (left) and adjoint errors $\|P_{1,ni} - p_1(t_{ni})\|_\infty$ (right), $n = 0, \dots, N - 1, i = 1, \dots, 4$.

where $h := 0.5/N$ with $N = 40, 80, 160, 320$. Note that $h_0 + \dots + h_{N-1} = 0.5$ for even N . In Figure 1, results for $\sigma = 1.0, 1.3, 1.5$ are presented. Since σ is constant, we have $\sigma = 1 + \eta_n h_n$ with $\eta_n = O(h_n^{-1})$, i.e., the non-smooth case. Results are shown in Figure 1. For the first state component y_1 , all methods works quite robust with respect to greater variations in the stepsize sequence. Order four for AP4o43vs is clearly visible, whereas the third-order schemes reach their order asymptotically from below. The symmetric scheme AP4o33vg performs significantly better than the other two third-order methods, which obviously have to pay a price for their larger stability angles α . This observation also applies to the first costate component p_1 . Here, the variations in the errors for different σ are significant. All methods converge with nearly fourth order for p_1 since $\tau^P = 0$, here.

Next, we choose a smoothly varying stepsize sequence with $\sigma_n = 1 + \eta h_n$, setting

$$h_0 = h, \quad h_n = \frac{h_{n-1}}{1 - \eta h_{n-1}}, \quad n = 1, 2, \dots, N - 1.$$

We use $h = (0.004, 0.002, 0.001, 0.0005)$ to mimic mesh refinement and set $\eta = 0.3$ to reach $T \approx 0.22$ for $N = 40, 80, 160, 320$. The resulting stepsize sequence is strictly increasing which leads to grids providing good approximations for the stiff part $\exp(-50t)$ of the state solution. Results are shown in Figure 2. The improvements over constant time steps, i.e. $\sigma = 1$, are clearly seen. The methods AP4o33va and AP4o33vs show their order three for the state y_1 for smaller time steps. Once again, AP4o33vg performs best among the third-order methods and has order three also for larger time steps. The fourth-order AP4o43vs benefits from its higher order and reaches full order four in the limit for large N . Order four for the costate p_1 shows up for smoothly varying σ_n by all methods, where the symmetric AP4o33vg comes quite close to AP4o43vs.

7.1.2 Error equidistributing stepsize sequences

To provide an optimized stepsize sequence a priori, we select $y(t)$ for grid construction following the error equidistribution principle introduced in [3, Chapter 9.1.1]. Due to the constant solutions $p_i(t), i = 1, 2, 3$, a well designed mesh for all components of the state vector y will work fine for p , too. Given an asymptotic behaviour of the global error, $\|y(t_n) - Y(t_n)\|_2 = O(h_n^r \|y^{(r)}(t_n)\|_2)$

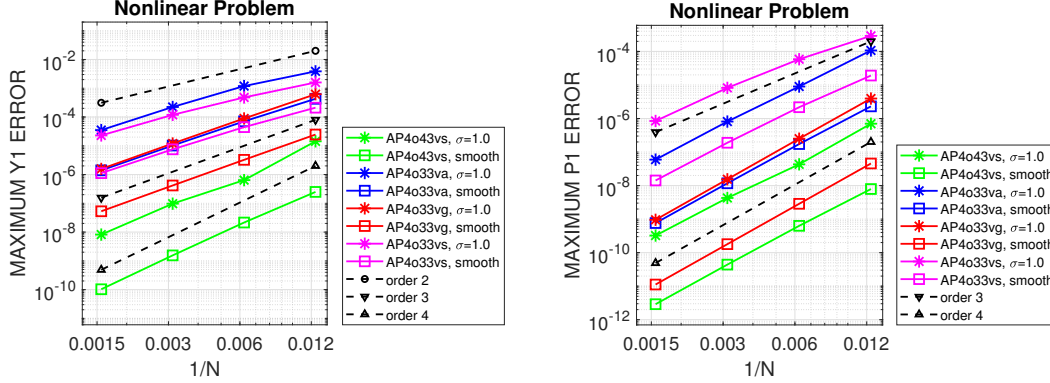


Figure 2: Test with smoothly varying $\sigma_n = 1 + 0.3h_n$ and final time $T \approx 0.22$, results for $\sigma_n \equiv 1$ are included. Convergence of the maximal state errors $\|Y_{1,ni} - y_1(t_{ni})\|_\infty$ (left) and adjoint errors $\|P_{1,ni} - p_1(t_{ni})\|_\infty$ (right), $n = 0, \dots, N - 1$, $i = 1, \dots, 4$.

with a numerical approximation Y and a global convergence order $r > 0$, a mesh density function $\psi(t) := \|y^{(r)}(t)\|_2^{1/r}$ is defined. Such a function has the property

$$\int_{t_n}^{t_{n+1}} \psi(t) dt \approx h_n \psi(t_n) = h_n \|y^{(r)}(t_n)\|_2^{1/r} \approx C \|y(t_n) - Y(t_n)\|_2^{1/r}. \quad (117)$$

The equidistribution of the global errors over a mesh $0 < t_1 < \dots < t_{N+1} = T = 0.5$ requires

$$\int_{t_n}^{t_{n+1}} \psi(t) dt = \frac{1}{N+1} \int_0^T \psi(t) dt = \text{const}. \quad (118)$$

For our case, we set

$$\psi(t) := \|y^{(r)}(t)\|_2^{1/r} = \left(\left(\lambda^r \exp(\lambda t) + r! (1-t)^{-(r+1)} \right)^2 + (\lambda^r \exp(\lambda t))^2 \right)^{\frac{1}{2r}} \quad (119)$$

with $r = 4$ for the fourth-order method AP4o43vs and $r = 3$ for the third-order schemes. The Euclidean norm is used here in order to obtain a smooth function ψ facilitating the solution of the following problem.

An efficient way to derive an optimized mesh is to define a continuous node distribution $x(\xi)$ as solution of a second-order boundary value problem [10, Chapter 2.2.2]

$$\partial_\xi (\psi(x(\xi)) \partial_\xi x(\xi)) = 0, \quad x(0) = 0, \quad x(0.5) = 0.5, \quad \xi \in [0, 0.5]. \quad (120)$$

To numerically solve this problem, we apply uniform linear finite elements with N inner nodes ξ_n , $n = 1, \dots, N$ and a pseudo-timestepping scheme. Finally, we set $t_n := x(\xi_n)$. We like to note that this procedure may also be applied with density functions ψ based on error *estimates*. However, this topic will be considered in a forthcoming paper. The optimized meshes for $N + 1 = 40, 80, 160, 320$ are shown in Figure 3. The corresponding minimum and maximum σ -values and maximum $|\eta|$ -values in $\sigma_n = 1 + \eta_n h_n$ for this grid sequence, denoted by $\underline{\sigma}$, $\bar{\sigma}$, $\bar{\eta}$, are

$$\begin{aligned} \underline{\sigma} &= (0.93, 0.96, 0.97, 0.98), \quad \bar{\sigma} = (1.31, 1.23, 1.15, 1.09), \quad \bar{\eta} = (16.6, 16.7, 18.2, 19.6), \quad \text{for } r = 3, \\ \underline{\sigma} &= (0.94, 0.97, 0.98, 0.99), \quad \bar{\sigma} = (1.24, 1.14, 1.08, 1.04), \quad \bar{\eta} = (12.5, 12.5, 12.5, 12.5), \quad \text{for } r = 4. \end{aligned}$$

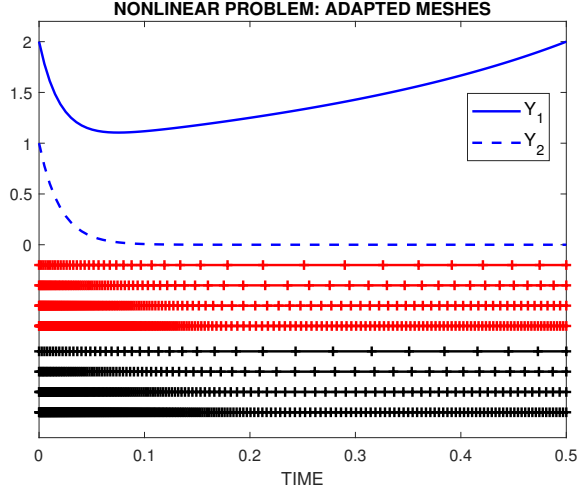


Figure 3: Functions $y_1(t) = (\exp(\lambda t) + (1-t)^{-1})$, $y_2(t) = \exp(\lambda t)$ with $\lambda = -50$ and adapted meshes for $r = 3$ (red), $r = 4$ (black) and $N + 1 = 40, 80, 160, 320$ time intervals (from top to bottom).

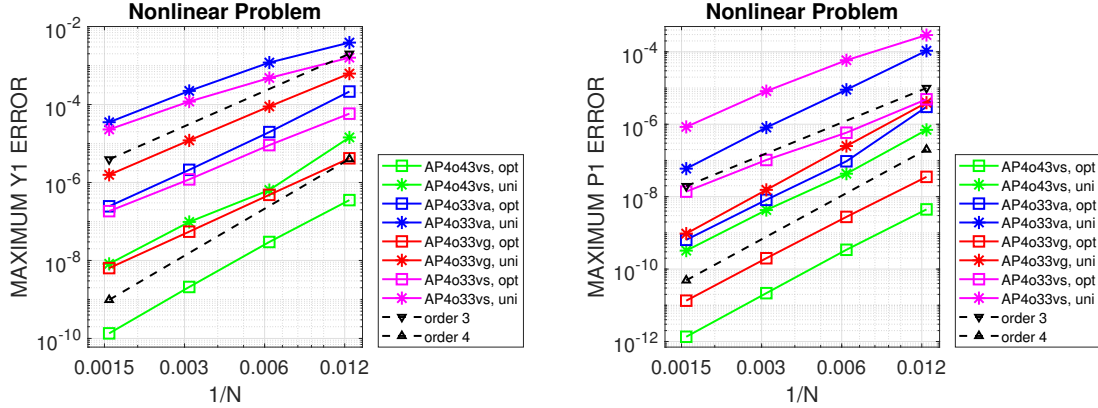


Figure 4: Test with adaptively chosen stepsizes, results for uniformly refined stepsizes are included. Convergence of the maximal state errors $\|Y_{1,ni} - y_1(t_{ni})\|_\infty$ (left) and adjoint errors $\|P_{1,ni} - p_1(t_{ni})\|_\infty$ (right), $n = 0, \dots, N$, $i = 1, \dots, 4$.

Obviously, for $r = 3$, the maximum constants $\bar{\eta}$ increase only slightly in each refinement step, characterizing a smooth stepsize sequence. A closer inspection reveals that $\max_n |\eta_n| < 20.4$ for arbitrary large n . For $r = 4$, we find $\max_n |\eta_n| \leq 12.5$.

Numerical results for the maximum state and adjoint errors of the first components y_1 and p_1 are presented in Figure 4. First of all, we observe for the state y_1 that the accuracy of all methods is improved by two orders of magnitude versus uniform refinement. This nicely demonstrates the potential of global error control by adaptive variable time steps. The achieved accuracy is still one order of magnitudes better than for the meshes in the former test with smoothly varying σ ,

since the latter one could be understood as a first improvement over uniform step sizes. The third-order methods show their order with clear advantage for AP4o33vg. The fourth-order method AP4o43vs asymptotically reaches order four as predicted by our convergence theory for smooth stepsize sequences. It beats the other triplets and the absolute values of the errors and therefore the quality of the numerical solutions are very impressive. The convergence orders for the costate p_1 are between three and four. The errors are much smaller than for y_1 . Once again, the symmetric AP4o33vg performs remarkably well and quite close to AP4o43vs.

7.2 The Catenary problem

The second problem is a modification of the „Linea Catenaria“ of the hanging rope [8, Chapter 1.3, Exercise 8]. The well-known solution $y(t) = \cosh(a_1 t + a_2)/a_1$ solves a second order differential equation, which we transform to a system of first order. The problem formulated as an optimal control problem of tracking type reads:

$$\begin{aligned} & \text{Minimize } y_3(2) \\ & \text{subject to } y_1'(t) = y_2(t), \\ & y_2'(t) = 0.5 a_1 (1 + y_2^2(t))^{1/2} + u(t), \\ & y_3'(t) = 0.5 (y_1(t) - y_d(t))^2 + 0.5 (u(t) - u_d(t))^2, \quad t \in (0, 2], \\ & y_1(0) = \cosh(a_2)/a_1, \quad y_2(0) = \sinh(a_2), \quad y_3(0) = 0, \end{aligned}$$

with $y_d(t) = \cosh(a_1 t + a_2)/a_1$ and $u_d(t) = 0.5 a_1 \cosh(a_1 t + a_2)$. The optimality condition

$$\nabla_u f(y, u)^\top p = p_2 + (u - u_d)p_3 = 0$$

with the adjoint variables $p = (p_1, p_2, p_3)^\top$ can be again used to calculate the optimal control from $u = u_d - p_2/p_3$, which together with the adjoint equations gives the boundary value problem (with eliminated control)

$$\begin{aligned} y_1'(t) &= y_2(t), \\ y_2'(t) &= 0.5 a_1 (1 + y_2^2(t))^{1/2} + u_d(t) - \frac{p_2(t)}{p_3(t)} \\ y_3'(t) &= 0.5 (y_1(t) - y_d(t))^2 + 0.5 \left(\frac{p_2(t)}{p_3(t)} \right)^2, \\ p_1'(t) &= - (y_1(t) - y_d(t)) p_3(t), \\ p_2'(t) &= - p_1(t) - 0.5 a_1 (1 + y_2^2(t))^{-1/2} y_2(t) p_2(t), \\ p_3'(t) &= 0, \quad t \in (0, 2], \\ y_1(0) &= \cosh(a_2)/a_1, \quad y_2(0) = \sinh(a_2), \quad y_3(0) = 0, \quad p_1(2) = 0, \quad p_2(2) = 0, \quad p_3(2) = 1. \end{aligned}$$

The exact solutions are $y_1(t) = \cosh(a_1 t + a_2)/a_1$, $y_2(t) = \sinh(a_1 t + a_2)$, $y_3(t) = 0$, $p_1(t) = p_2(t) \equiv 0$, $p_3(t) = 1$. The components $y_1(t)$ and $y_2(t)$ exhibit exponential boundary layer structures at $t = 0$ and $t = 2$. We choose $a_1 = 10$ and $a_2 = -10$ (mildly stiff regime).

We will show results for optimized meshes adapted to $y(t)$. Here, the mesh density function is defined as

$$\psi(t) := \|y^{(r)}(t)\|_2^{1/r} = \left(\left(a_1^{r-1} \cosh^{(r)}(a_1 t + a_2) \right)^2 + \left(a_1^r \sinh^{(r)}(a_1 t + a_2) \right) \right)^{\frac{1}{2r}} \quad (121)$$

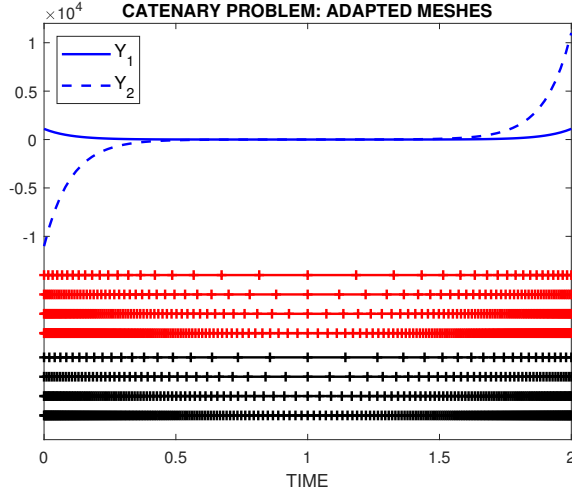


Figure 5: Functions $y_1(t) = 0.1 \cosh(10t - 10)$, $y_2(t) = \sinh(10t - 10)$ and adapted meshes for $r = 3$ (red), $r = 4$ (black) and $N + 1 = 40, 80, 160, 320$ time intervals (from top to bottom).

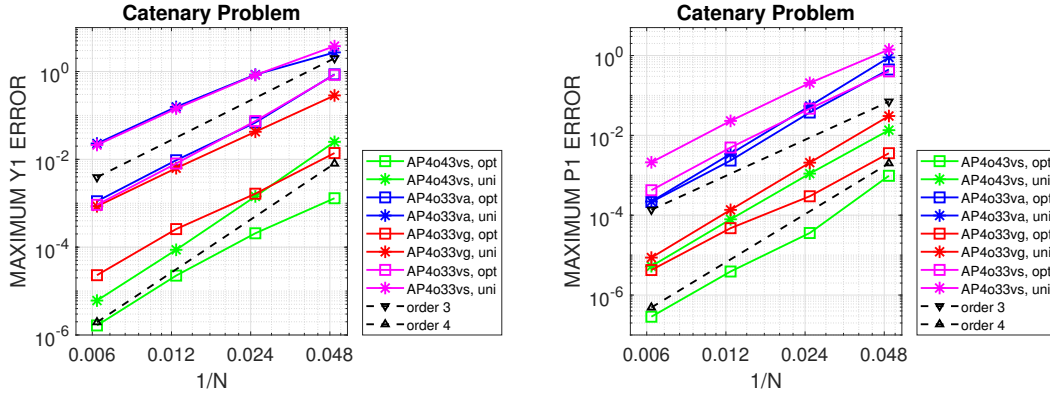


Figure 6: Test with adaptively chosen stepsizes, results for uniformly refined stepsizes are included. Convergence of the maximal state errors $\|Y_{1,ni} - y_1(t_{ni})\|_\infty$ (left) and adjoint errors $\|P_{1,ni} - p_1(t_{ni})\|_\infty$ (right), $n = 0, \dots, N$, $i = 1, \dots, 4$.

with $r = 4$ for the fourth-order method AP4o43vs and $r = 3$ for the third-order schemes. Solving the boundary value problem (120) for $N + 1 = 40, 80, 160, 320$, we get the optimized meshes shown in Figure 5. The corresponding minimum and maximum σ -values and maximum $|\eta|$ -values are

$$\underline{\sigma} = (0.74, 0.80, 0.86, 0.92), \quad \bar{\sigma} = (1.35, 1.25, 1.16, 1.09), \quad \bar{\eta} = (3.31, 3.33, 3.33, 3.33), \quad \text{for } r = 3,$$

$$\underline{\sigma} = (0.81, 0.87, 0.92, 0.96), \quad \bar{\sigma} = (1.24, 1.15, 1.08, 1.04), \quad \bar{\eta} = (2.49, 2.50, 2.50, 2.50), \quad \text{for } r = 4.$$

The maximum values $\max_n |\eta_n|$ are nearly constant such that all stepsize sequences are perfectly smooth.

Numerical results for the maximum state and adjoint errors of the first components y_1 and p_1

are presented in Figure 6. The improvement of the accuracy for the state y_1 on adapted meshes is clearly visible but less pronounced compared to the first test problem since the boundary layer is less marked here. All methods asymptotically reach their order three and four, respectively. AP4o33va and AP4o33vs perform equally well, whereas AP4o33vg is again the best third-order method by two orders of magnitude. The improvement of AP4o43vs is less pronounced, but the scheme delivers still the best results. The convergence orders for the costate p_1 is close to four. AP4o33vg and AP4o43vs are the best methods with advantage for the latter one.

8 Summary

We have constructed and analysed variable-stepsize implicit Peer triplets which can be applied to control problems with varying dynamics in the constraints of ODE type. Convergence results of s -stage Peer methods are proved for bounded or smoothly changing stepsize ratios. A notable theoretical result is that an LSRK-property (Last Stage is Runge-Kutta) leads to improved properties of the triplet. Balancing between good stability properties and small error constants, we have constructed three third-order methods: (1) the $A(61.59^\circ)$ -stable symmetric pulcherrima AP4o33vg with no smoothness restrictions on the stepsize ratios and very small error constants, (2) the $A(83.74^\circ)$ -stable AP4o33vs for smooth grids and with larger error constants, (3) the $A(90^\circ)$ -stable AP4o33va for smooth grids and still moderate error constants, especially suitable for dynamical systems with eigenvalues close to or on the imaginary axis. We could also find the $A(74.015^\circ)$ -stable AP4o43vs, which has order four for the state variables with a very small error constant, if applied with smooth grids. All the methods show their theoretical order in our numerical tests. The higher-order AP4o43vs always gives the best results, but also our pulcherrima triplet AP4o33vg performs surprisingly well and beats all other third-order methods.

In future work, we will discuss for three of the Peer triplets from this paper the integration of automatic grid construction in efficient gradient-based solution algorithms for the fully coupled optimal control problem with unknown control u and further constraints, where positivity of the quadrature weights in K is required.

Acknowledgements. The first author is supported by the Deutsche Forschungsgemeinschaft (DFG, German Research Foundation) within the collaborative research center TRR154 “*Mathematical modeling, simulation and optimisation using the example of gas networks*” (Project-ID 239904186, TRR154/3-2022, TP B01).

A Coefficients of all Peer triplets

Although all data for the 4-stage Peer triplets from the text are known exactly with long rational or algebraic expressions we display most of them as real numbers in double precision due to space limitations. The essential data are the node vector $\mathbf{c}^T = (c_1, c_2, c_3, c_4)$, the coefficients (A_0, K_0) , (A, K) , (A_N, K_N) of the starting, the standard and the end step and the free coefficients of the sparse matrix

$$\hat{B}(\sigma) = \begin{pmatrix} 1 & 1 & 1 & \hat{a}_{14} \\ 0 & 0 & 0 & \hat{b}_{24}(\sigma) \\ 0 & 0 & 0 & \hat{b}_{34}(\sigma) \\ \hat{a}_{41} & \hat{b}_{41}(\sigma) & \hat{b}_{43}(\sigma) & \hat{b}_{44}(\sigma) \end{pmatrix}$$

depending on the stepsize ratio σ . Although not required for the implementation of the triplets we also present the weight matrices W in order to enable verification of uniform zero stability (65). All other coefficients may be computed by

$$a = A_0 \mathbf{1}, \quad w = A_N^T \mathbf{1}, \quad B(\sigma) = V_4^{-T} \hat{B}(\sigma) V_4,$$

where $V_4 = (\mathbf{1}, \mathbf{c}, \mathbf{c}^2, \mathbf{c}^3)$ is the Vandermonde matrix for the nodes from \mathbf{c} .

A1: Coefficients of AP4o33vg

$$\mathbf{c}^T = \left(0, \frac{1}{3}, \frac{2}{3}, 1\right), \quad K_0 = K = K_N = \text{diag} \left(\frac{1}{8}, \frac{3}{8}, \frac{3}{8}, \frac{1}{8}\right),$$

$$A_0 = \begin{pmatrix} \frac{49}{80} & \frac{3}{4} & -\frac{3}{16} & 0 \\ -\frac{87}{80} & 0 & \frac{9}{16} & 0 \\ \frac{87}{80} & -\frac{9}{4} & \frac{27}{16} & 0 \\ -\frac{49}{80} & \frac{3}{2} & -\frac{33}{16} & 1 \end{pmatrix}, \quad A = \begin{pmatrix} 1 & 0 & 0 & 0 \\ -\frac{9}{4} & \frac{9}{4} & 0 & 0 \\ \frac{9}{4} & -\frac{9}{2} & \frac{9}{4} & 0 \\ -1 & \frac{9}{4} & -\frac{9}{4} & 1 \end{pmatrix}, \quad A_N = \begin{pmatrix} 1 & 0 & 0 & 0 \\ -\frac{33}{16} & \frac{27}{16} & \frac{9}{16} & -\frac{3}{16} \\ \frac{3}{2} & -\frac{9}{4} & 0 & \frac{3}{4} \\ -\frac{49}{80} & \frac{87}{80} & -\frac{87}{80} & \frac{49}{80} \end{pmatrix},$$

$$\hat{B}(\sigma) = \begin{pmatrix} 1 & 1 & 1 & 1 \\ 0 & 0 & 0 & \frac{1}{36\sigma} \\ 0 & 0 & 0 & 0 \\ 0 & \frac{\sigma}{36} & \frac{\sigma}{18} & \frac{13}{1340} + \frac{\sigma^2}{20} \end{pmatrix}, \quad W = \begin{pmatrix} 1 & -2 & \frac{24}{5} & -\frac{9}{2} \\ 1 & -\frac{4}{3} & 0 & \frac{3}{2} \\ 1 & -\frac{2}{3} & -\frac{8}{5} & \frac{3}{2} \\ 1 & 0 & 0 & 0 \end{pmatrix}.$$

A2: Coefficients of AP4o33vs

$$\mathbf{c}^T = \left(\frac{144997}{389708}, \frac{73}{748}, \frac{77297572}{117896267}, 1\right),$$

$$K_n = \text{diag}(0.2089552772313791, 0.2461266069992848, 0.4259606950456414, 0.1189574207236947)$$

for $n = 0, \dots, N$,

$$A_0 = \begin{pmatrix} 2.773177556033415 & -5.711973424498560 & -0.4047906551114346 & 0 \\ -0.2775983738279357 & 2.618694207814551 & 0.1431328584722113 & 0 \\ -5.101798226146757 & 4.755733335146421 & 2.836975327925722 & 0 \\ 2.606219043941277 & -1.662454118462412 & -2.575317531286499 & 1 \end{pmatrix},$$

$$A = \begin{pmatrix} 0.7588470158140062 & 0 & 0 & 0 \\ 0.4346633458753195 & 0.5989561692950702 & 0 & 0 \\ -3.295204661275873 & -0.3671669165116753 & 2.473930545531403 & 0 \\ 2.101694299586548 & -0.2317892527833949 & -2.473930545531403 & 1 \end{pmatrix},$$

$A_N =$

$$\begin{pmatrix} 0.7588470158140062 & 0 & 0 & 0 \\ 0.1098911012176018 & 0.7137947386723661 & 0.2912786335371730 & -0.08134495825675107 \\ -1.064925547930965 & -1.155787455679128 & 0.4736590838298028 & 0.5586128875241437 \\ 1.474979453185272 & -0.01018461275608742 & -1.911848510874736 & 0.8430281717173012 \end{pmatrix},$$

$$\begin{aligned}
\hat{a}_{14} &= 1, \hat{b}_{24} = 0.02321239244678227/\sigma, \hat{b}_{34} = 0, \\
\hat{a}_{41} &= 0.1010743874247749, \hat{b}_{42} = \hat{a}_{41} + 0.003586671392069201 \sigma, \\
\hat{b}_{43} &= \hat{a}_{41} + 0.007173342784138403 \sigma - 0.002465255918355442 \sigma^2, \\
\hat{b}_{44} &= 0.0078782707622298066 + 0.1683589306029579 \sigma - 0.1125 \sigma^2 + 0.025 \sigma^3,
\end{aligned}$$

$$W = \begin{pmatrix} 1 & -\frac{49}{3} & -4 & 27 \\ 1 & -\frac{47}{2} & 33 & -\frac{95}{3} \\ 1 & -9 & -\frac{52}{3} & \frac{119}{5} \\ 1 & 0 & 0 & 0 \end{pmatrix}.$$

A3: Coefficients of AP4o43vs

$$\mathbf{c}^\top = \left(\frac{1}{2}(7 - \sqrt{29}), \frac{1}{2}, \frac{1}{10}(3 + \sqrt{29}), 1 \right),$$

$K_0 =$

$$\begin{pmatrix} 0.5 & 1 & 0 & 0 \\ -1.120097818618729 & -3.509114262220923 & 0.02331113741482591 & -0.07507889931006730 \\ 1.951080835579074 & 6.817902173284554 & 0.04964515498231075 & 0.2324661353733601 \\ -1.097482134196919 & -3.777428018384294 & 0.04886693226626865 & -0.04407123616946104 \end{pmatrix},$$

$A_0 =$

$$\begin{pmatrix} -2.258093793670717 & 1.862197768561405 & 0.8958960251093118 & 0 \\ 11.58487375982880 & -4.941113522467058 & -3.725846848775559 & -0.02162218680256198 \\ -21.42711527957095 & 7.401740825625927 & 8.196612369685553 & 0.2072923201571290 \\ 12.10033531341286 & -4.322825071720274 & -5.366661546019306 & 0.8143298666454331 \end{pmatrix}$$

$$K = \text{diag}(0.2392605543426944, 0.5076556795243664, 0.1624309662178738, 0.09065279991506543),$$

$$A = \begin{pmatrix} 2.932991332809296 & 0 & 0 & 0 \\ -9.722226151163717 & 2.605421230471736 & 0 & 0 \\ 15.03085810481218 & -5.510604377851853 & 2.011734286390463 & 0 \\ -8.241623286457758 & 2.905183147380117 & -2.011734286390463 & 1 \end{pmatrix},$$

$$\begin{aligned}
\hat{a}_{14} &= 1, \hat{b}_{24} = 0.006728479970272900/\sigma, \hat{b}_{34} = 0, \\
\hat{a}_{41} &= -0.4373259052924791, \hat{b}_{42} = \hat{a}_{41} + 0.0007142621905395870 \sigma, \\
\hat{b}_{43} &= \hat{a}_{41} + 0.001428524381079174 \sigma + 0.005699612131335000 \sigma^2, \\
\hat{b}_{44} &= \hat{a}_{41} + 0.002142786571618761 \sigma - 0.01091141501818702 \sigma^2 + 0.01709883639400500 \sigma^3.
\end{aligned}$$

A weight matrix W with short rationals is given by (92).

$$K_N = \begin{pmatrix} 0.3352224422310586 & 0.6666666666666666 & 0.25 & 0 \\ -0.4081466631436265 & -2.243551054735366 & -0.9919828228000089 & -0.01618666259097973 \\ 0.7502573728050319 & 4.650087123227831 & 1.851360793436682 & 0.05011862096669070 \\ -0.4323129259705010 & -2.589251268789736 & -0.9063392628643313 & 0.03405764156058810 \end{pmatrix},$$

$$A_N = \begin{pmatrix} 2.133506902525376 & -1.201712432255361 & 2.001196862539281 & 0 \\ -6.352860439191028 & 7.343234398037428 & -8.042312319130696 & -0.06486656040768594 \\ 9.042449972383633 & -12.89903567845361 & 14.76669675894938 & 0.6218769604713869 \\ -4.823096435717981 & 6.757513712671541 & -8.725581302357963 & 0.4429895999362990 \end{pmatrix}.$$

A4: Coefficients of AP4o33va

$$\mathbf{c}^\top = \left(0, \frac{53}{34}, \frac{6242}{30453}, \frac{298}{153} \right),$$

$$K_0 = \begin{pmatrix} -0.07894736842105263 & -0.3541666666666667 & 0.8 & 0 \\ -0.5092967024450286 & -0.05954441426546966 & 1.5 & 0 \\ -0.2793212824140483 & 0.4819625026869399 & 0.01024569899875302 & 0 \\ 0.4370032270471419 & 0.2582293704863321 & -1.071186604429968 & \kappa_{44}^{(0)} \end{pmatrix},$$

$$A_0 = \begin{pmatrix} -2.845147129315054 & -0.4034338322824405 & 4.858078566685144 & 0 \\ -3.334526877014251 & 0.1129706979359890 & 3.683717732206632 & 0 \\ 2.756370844715334 & 0.6933008415389270 & -4.233985411744457 & 0 \\ 2.572062980946981 & 0.3827708538751709 & -2.987953672161328 & a_{44}^{(0)} \end{pmatrix},$$

where $\kappa_{44}^{(0)} = -0.13497776057693290$, $a_{44}^{(0)} = -0.2542255953866471$.

$$K = \text{diag}(-0.4305621262329876, 0.32648079224113569, 1.239059094568785, -0.1349777605769329),$$

$$A = \begin{pmatrix} -6.403144243666246 & 0 & 0 & 0 \\ -6.032436530257817 & 0.4188810164603250 & 0 & 0 \\ 7.334872792461045 & 0.1741541060226739 & 2.017487387419302 & 0 \\ 4.249467800796027 & 0.1925734385846475 & -0.6976301724333114 & -0.2542255953866471 \end{pmatrix},$$

$$\hat{a}_{14} = 1.108695652173913, \hat{b}_{24} = -0.4962124378026289 / \sigma, \hat{b}_{34} = -0.6391248143857920 / \sigma^2,$$

$$\hat{a}_{41} = 4.607142857142857, \hat{b}_{42} = \hat{a}_{41} - 0.2679484769093443 \sigma, \hat{b}_{43} = \hat{a}_{41} - 0.5358969538186886 \sigma,$$

$$\hat{b}_{44} = -\frac{2198}{55} + \frac{1607}{22} \sigma - \frac{147}{5} \sigma^2,$$

$$W = \begin{pmatrix} 1 & -2 & 6 & 2.509523385281405 \\ 1 & 1.117647058823529 & 12.32698961937716 & 7.052310433008046 \\ 1 & -1.590056808852987 & 1.836922096090924 & 0.5167228373603610 \\ 1 & 1.895424836601307 & 27.53940792003076 & 16.07292401233786 \end{pmatrix}$$

$$K_N = \begin{pmatrix} -0.4305621262329876 & 0 & 0 & 0 \\ -0.7584777455167840 & -0.4907990379996561 & 0.6666666666666667 & 0.9090909090909091 \\ -0.4295489737333543 & 0.09171637742180421 & 1.7797533837522101 & -0.2028616928718752 \\ 0.6522412050328370 & 0.3192953012669550 & -0.51790142522729154 & -0.5886128416494334 \end{pmatrix},$$

$$A_N = \begin{pmatrix} -6.4031442436662458 & 0 & 0 & 0 \\ -0.95260517222681956 & 1.865037832767615 & -6 & -0.5259881743382867 \\ 6.79592553738488869 & 0.3023172450424132 & 2.591223325518416 & -0.1629518220426969 \\ 0.525998613319805586 & -0.7619282537426990 & 3.676768004714683 & 0.04934710726892677 \end{pmatrix}$$

References

- [1] G. Albi, M. Herty, and L. Pareschi. Linear multistep methods for optimal control problems and applications to hyperbolic relaxation systems. *Applied Mathematics and Computation*, 354:460–477, 2019.
- [2] I. Almuslimani and G. Vilmart. Explicit stabilized integrators for stiff optimal control problems. *SIAM J. Sci. Comput.*, 43:A721–A743, 2021.
- [3] U.M. Ascher, R.M.M. Mattheij, and R.D. Russell. *Numerical Solution of Boundary Value Problems for Ordinary Differential Equations*. Society for Industrial and Applied Mathematics, 1995.
- [4] D. Beigel, M.S. Mommer, L. Wirsching, and H.G. Bock. Approximation of weak adjoints by reverse automatic differentiation of BDF methods. *Numer. Math.*, 126:383–412, 2014.
- [5] V.D. Blondel and Y. Nesterov. Polynomial-time computation of the joint spectral radius for some sets of nonnegative matrices. *SIAM J. Matrix Anal. Appl.*, 31:865–876, 2010.
- [6] F.J. Bonnans and J. Laurent-Varin. Computation of order conditions for symplectic partitioned Runge-Kutta schemes with application to optimal control. *Numer. Math.*, 103:1–10, 2006.
- [7] W.W. Hager. Runge-Kutta methods in optimal control and the transformed adjoint system. *Numer. Math.*, 87:247–282, 2000.
- [8] E. Hairer, S. P. Nørsett, and G. Wanner. *Solving Ordinary Differential Equations I*. Springer-Verlag, New York, 2006.
- [9] M. Herty, L. Pareschi, and S. Steffensen. Implicit-explicit Runge-Kutta schemes for numerical discretization of optimal control problems. *SIAM J. Numer. Anal.*, 51:1875–1899, 2013.
- [10] W. Huang and R.D. Russell. *Adaptive Moving Mesh Methods*. Springer New York, Dordrecht, Heidelberg, London, 2011.
- [11] J. Lang and B.A. Schmitt. Discrete adjoint implicit peer methods in optimal control. *J. Comput. Appl. Math.*, 416:114596, 2022.

- [12] J. Lang and B.A. Schmitt. Implicit A-stable peer triplets for ODE constrained optimal control problems. *Algorithms*, 15:310, 2022.
- [13] J. Lang and B.A. Schmitt. Exact discrete solutions of boundary control problems for the 1D heat equation. *J. Optim. Theory Appl.*, 196:1106–1118, 2023.
- [14] X. Liu and J. Frank. Symplectic Runge-Kutta discretization of a regularized forward-backward sweep iteration for optimal control problems. *J. Comput. Appl. Math.*, 383:113133, 2021.
- [15] B.A. Schmitt. Algebraic criteria for A-stability of peer two-step methods. Technical Report arXiv:1506.05738, 2015.
- [16] B.A. Schmitt and R. Weiner. Efficient A-stable peer two-step methods. *J. Comput. Appl. Math.*, pages 319–32, 2017.
- [17] B.A. Schmitt, R. Weiner, and K. Erdmann. Implicit parallel peer methods for stiff initial value problems. *Appl. Numer. Math.*, 53:457–470, 2005.
- [18] D. Schröder, J. Lang, and R. Weiner. Stability and consistency of discrete adjoint implicit peer methods. *J. Comput. Appl. Math.*, 262:73–86, 2014.
- [19] J.L. Troutman. *Variational Calculus and Optimal Control*. Springer, New York, 1996.
- [20] Y. Xu. A characterization of positive quadrature formulae. *Math. Comp.*, 62:703–718, 1994.